Scalar self-force for generic, bound orbits on Kerr

Zachary Nasipak[1]
w/ Thomas Osburn[2] and Charles R. Evans[1]

June 20, 2017

[1]University of North Carolina–Chapel Hill

[2]Oxford College of Emory University

EMRIs, gravitational self-force & perturbation theory

Extreme-mass-ratio inspirals (EMRIs)

- eLISA sources
- Small mass ratio $\mu \ll M \Rightarrow$ black hole perturbation theory (BHPT)
- Deviations from geodesic motion sourced by gravitational self-force (GSF)

$$F^{\alpha}_{\text{SSF}}\left[\Phi^R/\mathcal{A}^R_{\alpha}/h^R_{\mu\nu}\right] = u^{\beta}\nabla_{\beta}\left(\mu u^{\alpha}\right)$$

GSF applications

- More accurate long-term inspirals

$$\phi = \kappa_{-1}\left(\frac{\mu}{M}\right)^{-1} + \kappa_{-1/2}\left(\frac{\mu}{M}\right)^{-1/2} + \kappa_0\left(\frac{\mu}{M}\right)^{0} + \cdots$$

- Leading order GSF contributes to κ_{-1} & κ_0
- Required phase accuracy ~ 0.1 radians $\Rightarrow 7-8$ digits

EMRIs, gravitational self-force & perturbation theory

Extreme-mass-ratio inspirals (EMRIs)

- eLISA sources
- Small mass ratio $\mu \ll M \Rightarrow$ black hole perturbation theory (BHPT)
- Deviations from geodesic motion sourced by gravitational self-force (GSF)

$$F^{\alpha}_{\mathrm{SSF}}\left[\Phi^R/\mathcal{A}^R_{\alpha}/h^R_{\mu\nu}\right] = u^{\beta}\nabla_{\beta}\left(\mu u^{\alpha}\right)$$

GSF applications

- More accurate long-term inspirals

$$\phi = \kappa_{-1}\left(\frac{\mu}{M}\right)^{-1} + \kappa_{-1/2}\left(\frac{\mu}{M}\right)^{-1/2} + \kappa_{0}\left(\frac{\mu}{M}\right)^{0} + \cdots$$

- Leading order GSF contributes to κ_{-1} & κ_0
- Required phase accuracy ~ 0.1 radians $\Rightarrow 7-8$ digits

EMRIs, gravitational self-force & perturbation theory

Extreme-mass-ratio inspirals (EMRIs)

- eLISA sources
- Small mass ratio $\mu \ll M \Rightarrow$ black hole perturbation theory (BHPT)
- Deviations from geodesic motion sourced by gravitational self-force (GSF)

$$F^{\alpha}_{\mathrm{SSF}}\left[\Phi^R/\mathcal{A}^R_{\alpha}/h^R_{\mu\nu}\right] = u^{\beta}\nabla_{\beta}\left(\mu u^{\alpha}\right)$$

GSF applications

- More accurate long-term inspirals

$$\phi = \kappa_{-1}\left(\frac{\mu}{M}\right)^{-1} + \kappa_{-1/2}\left(\frac{\mu}{M}\right)^{-1/2} + \kappa_0\left(\frac{\mu}{M}\right)^{0} + \cdots$$

- Leading order GSF contributes to κ_{-1} & κ_0
- Required phase accuracy ~ 0.1 radians $\Rightarrow 7-8$ digits

EMRIs, gravitational self-force & perturbation theory

Extreme-mass-ratio inspirals (EMRIs)

- eLISA sources
- Small mass ratio $\mu \ll M \Rightarrow$ black hole perturbation theory (BHPT)
- Deviations from geodesic motion sourced by gravitational self-force (GSF)

$$F^{\alpha}_{\mathrm{SSF}}\left[\Phi^{R}/\mathcal{A}^{R}_{\alpha}/h^{R}_{\mu\nu}\right] = u^{\beta}\nabla_{\beta}\left(\mu u^{\alpha}\right)$$

GSF applications

- More accurate long-term inspirals

$$\phi = \kappa_{-1}\left(\frac{\mu}{M}\right)^{-1} + \kappa_{-1/2}\left(\frac{\mu}{M}\right)^{-1/2} + \kappa_{0}\left(\frac{\mu}{M}\right)^{0} + \cdots$$

- Leading order GSF contributes to κ_{-1} & κ_0
- Required phase accuracy ~ 0.1 radians $\Rightarrow 7-8$ digits

EMRIs, gravitational self-force & perturbation theory

Extreme-mass-ratio inspirals (EMRIs)

- eLISA sources
- Small mass ratio $\mu \ll M \Rightarrow$ black hole perturbation theory (BHPT)
- Deviations from geodesic motion sourced by gravitational self-force (GSF)

$$F^{\alpha}_{\text{SSF}}\left[\Phi^R/\mathcal{A}^R_\alpha/h^R_{\mu\nu}\right] = u^\beta \nabla_\beta \left(\mu u^\alpha\right)$$

$$F^{\text{disp}}_\alpha(\tau) = \frac{1}{2}\left[F^{\text{ret}}_\alpha(\tau) - F^{\text{adv}}_\alpha(\tau)\right]$$

$$F^{\text{cons}}_\alpha(\tau) = \frac{1}{2}\left[F^{\text{ret}}_\alpha(\tau) + F^{\text{adv}}_\alpha(\tau)\right]$$

GSF applications

- More accurate long-term inspirals

$$\phi = \kappa_{-1}\left(\frac{\mu}{M}\right)^{-1} + \kappa_{-1/2}\left(\frac{\mu}{M}\right)^{-1/2} + \kappa_0\left(\frac{\mu}{M}\right)^{0} + \cdots$$

- Leading order GSF contributes to κ_{-1} & κ_0
- Required phase accuracy ~ 0.1 radians $\Rightarrow 7-8$ digits

EMRIs, gravitational self-force & perturbation theory

Extreme-mass-ratio inspirals (EMRIs)

- eLISA sources
- Small mass ratio $\mu \ll M \Rightarrow$ black hole perturbation theory (BHPT)
- Deviations from geodesic motion sourced by gravitational self-force (GSF)

$$F^{\alpha}_{\text{SSF}}\left[\Phi^R/\mathcal{A}^R_\alpha/h^R_{\mu\nu}\right] = u^\beta \nabla_\beta \left(\mu u^\alpha\right)$$

GSF applications

- More accurate long-term inspirals

$$\phi = \kappa_{-1}\left(\frac{\mu}{M}\right)^{-1} + \kappa_{-1/2}\left(\frac{\mu}{M}\right)^{-1/2} + \kappa_0\left(\frac{\mu}{M}\right)^{0} + \cdots$$

- Leading order GSF contributes to κ_{-1} & κ_0
- Required phase accuracy ~ 0.1 radians $\Rightarrow 7-8$ digits

$$F^{\text{disp}}_\alpha(\tau) = \frac{1}{2}\left[F^{\text{ret}}_\alpha(\tau) - \epsilon_{(\alpha)}F^{\text{ret}}_\alpha(-\tau)\right]$$

$$F^{\text{cons}}_\alpha(\tau) = \frac{1}{2}\left[F^{\text{ret}}_\alpha(\tau) + \epsilon_{(\alpha)}F^{\text{ret}}_\alpha(-\tau)\right]$$

EMRIs, gravitational self-force & perturbation theory

Extreme-mass-ratio inspirals (EMRIs)

- eLISA sources
- Small mass ratio $\mu \ll M \Rightarrow$ black hole perturbation theory (BHPT)
- Deviations from geodesic motion sourced by gravitational self-force (GSF)

$$F^{\alpha}_{\mathrm{SSF}}\left[\Phi^R / \mathcal{A}^R_\alpha / h^R_{\mu\nu}\right] = u^\beta \nabla_\beta \left(\mu u^\alpha\right)$$

GSF applications

- More accurate long-term inspirals

$$\phi = \kappa_{-1}\left(\frac{\mu}{M}\right)^{-1} + \kappa_{-1/2}\left(\frac{\mu}{M}\right)^{-1/2} + \kappa_0\left(\frac{\mu}{M}\right)^{0} + \cdots$$

- Leading order GSF contributes to κ_{-1} & κ_0
- Required phase accuracy ~ 0.1 radians $\Rightarrow 7 - 8$ digits

$$F^{\mathrm{disp}}_\alpha(\tau) = \frac{1}{2}\left[F^{\mathrm{ret}}_\alpha(\tau) - \epsilon_{(\alpha)} F^{\mathrm{ret}}_\alpha(-\tau)\right]$$

$$F^{\mathrm{cons}}_\alpha(\tau) = \frac{1}{2}\left[F^{\mathrm{ret}}_\alpha(\tau) + \epsilon_{(\alpha)} F^{\mathrm{ret}}_\alpha(-\tau)\right]$$

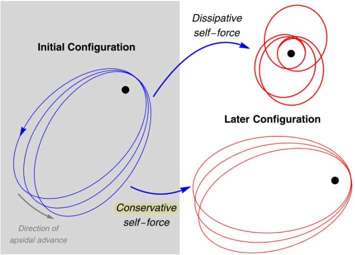

Image from Osburn (2016) **PRD 93**

EMRIs, gravitational self-force & perturbation theory

Extreme-mass-ratio inspirals (EMRIs)

- eLISA sources
- Small mass ratio $\mu \ll M \Rightarrow$ black hole perturbation theory (BHPT)
- Deviations from geodesic motion sourced by gravitational self-force (GSF)

$$F^\alpha_{\mathrm{SSF}}\left[\Phi^R / \mathcal{A}^R_\alpha / h^R_{\mu\nu}\right] = u^\beta \nabla_\beta \left(\mu u^\alpha\right)$$

GSF applications

- More accurate long-term inspirals

$$\phi = \kappa_{-1}\left(\frac{\mu}{M}\right)^{-1} + \kappa_{-1/2}\left(\frac{\mu}{M}\right)^{-1/2} + \kappa_0\left(\frac{\mu}{M}\right)^{0} + \cdots$$

- Leading order GSF contributes to κ_{-1} & κ_0
- Required phase accuracy ~ 0.1 radians $\Rightarrow 7-8$ digits

$$F^{\mathrm{disp}}_\alpha(\tau) = \frac{1}{2}\left[F^{\mathrm{ret}}_\alpha(\tau) - \epsilon_{(\alpha)} F^{\mathrm{ret}}_\alpha(-\tau)\right]$$

$$F^{\mathrm{cons}}_\alpha(\tau) = \frac{1}{2}\left[F^{\mathrm{ret}}_\alpha(\tau) + \epsilon_{(\alpha)} F^{\mathrm{ret}}_\alpha(-\tau)\right]$$

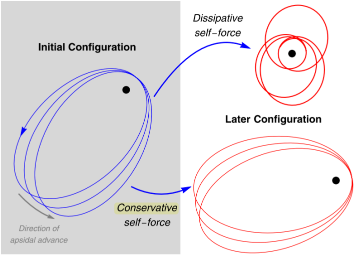

Image from Osburn (2016) **PRD 93**

EMRIs, gravitational self-force & perturbation theory

Extreme-mass-ratio inspirals (EMRIs)

- eLISA sources
- Small mass ratio $\mu \ll M \Rightarrow$ black hole perturbation theory (BHPT)
- Deviations from geodesic motion sourced by gravitational self-force (GSF)

$$F^{\alpha}_{\mathrm{SSF}}\left[\Phi^R/\mathcal{A}^R_\alpha/h^R_{\mu\nu}\right] = u^\beta \nabla_\beta \left(\mu u^\alpha\right)$$

GSF applications

- More accurate long-term inspirals

$$\phi = \kappa_{-1}\left(\frac{\mu}{M}\right)^{-1} + \kappa_{-1/2}\left(\frac{\mu}{M}\right)^{-1/2} + \kappa_0\left(\frac{\mu}{M}\right)^{0} + \cdots$$

- Leading order GSF contributes to κ_{-1} & κ_0
- Required phase accuracy ~ 0.1 radians $\Rightarrow 7-8$ digits

$$F^{\mathrm{disp}}_\alpha(\tau) = \frac{1}{2}\left[F^{\mathrm{ret}}_\alpha(\tau) - \epsilon_{(\alpha)} F^{\mathrm{ret}}_\alpha(-\tau)\right]$$

$$F^{\mathrm{cons}}_\alpha(\tau) = \frac{1}{2}\left[F^{\mathrm{ret}}_\alpha(\tau) + \epsilon_{(\alpha)} F^{\mathrm{ret}}_\alpha(-\tau)\right]$$

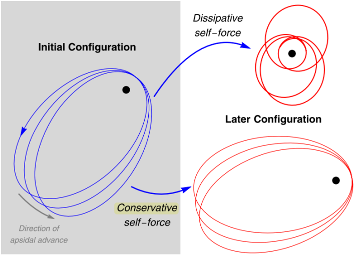

Image from Osburn (2016) **PRD 93**

EMRIs, gravitational self-force & perturbation theory

Extreme-mass-ratio inspirals (EMRIs)

- eLISA sources
- Small mass ratio $\mu \ll M \Rightarrow$ black hole perturbation theory (BHPT)
- Deviations from geodesic motion sourced by gravitational self-force (GSF)

$$F^{\alpha}_{\text{SSF}}\left[\Phi^R/\mathcal{A}^R_{\alpha}/h^R_{\mu\nu}\right] = u^{\beta}\nabla_{\beta}\left(\mu u^{\alpha}\right)$$

GSF applications

- More accurate long-term inspirals

$$\phi = \kappa_{-1}\left(\frac{\mu}{M}\right)^{-1} + \kappa_{-1/2}\left(\frac{\mu}{M}\right)^{-1/2} + \kappa_{0}\left(\frac{\mu}{M}\right)^{0} + \cdots$$

- Leading order GSF contributes to κ_{-1} & κ_0
- Required phase accuracy ~ 0.1 radians $\Rightarrow 7-8$ digits

$$F^{\text{disp}}_{\alpha}(\tau) = \frac{1}{2}\left[F^{\text{ret}}_{\alpha}(\tau) - \epsilon_{(\alpha)}F^{\text{ret}}_{\alpha}(-\tau)\right]$$

$$F^{\text{cons}}_{\alpha}(\tau) = \frac{1}{2}\left[F^{\text{ret}}_{\alpha}(\tau) + \epsilon_{(\alpha)}F^{\text{ret}}_{\alpha}(-\tau)\right]$$

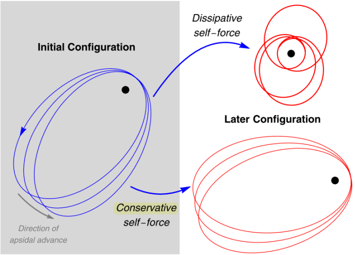

Image from Osburn (2016) **PRD 93**

EMRIs, gravitational self-force & perturbation theory

Extreme-mass-ratio inspirals (EMRIs)

- eLISA sources
- Small mass ratio $\mu \ll M \Rightarrow$ black hole perturbation theory (BHPT)
- Deviations from geodesic motion sourced by gravitational self-force (GSF)

$$F^{\alpha}_{\mathrm{SSF}}\left[\Phi^R/\mathcal{A}^R_\alpha/h^R_{\mu\nu}\right] = u^\beta \nabla_\beta\left(\mu u^\alpha\right)$$

GSF applications

- More accurate long-term inspirals

$$\phi = \kappa_{-1}\left(\frac{\mu}{M}\right)^{-1} + \kappa_{-1/2}\left(\frac{\mu}{M}\right)^{-1/2} + \kappa_0\left(\frac{\mu}{M}\right)^{0} + \quad \cdots$$

- Leading order GSF contributes to κ_{-1} & κ_0
- Required phase accuracy ~ 0.1 radians $\Rightarrow 7-8$ digits

$$F^{\mathrm{disp}}_\alpha(\tau) = \frac{1}{2}\left[F^{\mathrm{ret}}_\alpha(\tau) - \epsilon_{(\alpha)}F^{\mathrm{ret}}_\alpha(-\tau)\right]$$

$$F^{\mathrm{cons}}_\alpha(\tau) = \frac{1}{2}\left[F^{\mathrm{ret}}_\alpha(\tau) + \epsilon_{(\alpha)}F^{\mathrm{ret}}_\alpha(-\tau)\right]$$

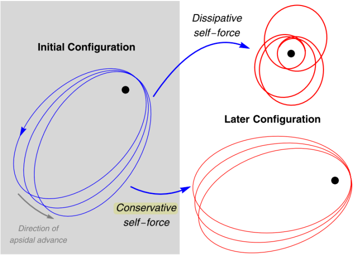

Image from Osburn (2016) **PRD 93**

Scalar self-force (SSF) as a toy model

SSF on Schwarzschild

- Circular geodesics

  Burko (2000) **PRL 84**: Freq. Domain (FD)

  Diaz-Rivera et al. (2004) **PRD 70**: FD

  Vega & Detweiler (2008) **PRD 77**: Time Domain (TD)

  Vega et al. (2009) **PRD 80**: TD

  Dolan & Barack (2011) **PRD 83**: TD

- Eccentric geodesics

  Haas (2007) **PRD 75**: TD

  Canizares et al. (2010) **PRD 82**: TD

  Diener et al. (2012) **PRL 102**: Effective source, TD

  Wardell et al. (2014) **PRD 89**: TD

SSF on Kerr

- Circular, equatorial geodesics

  Warburton & Barack (2010) **PRD 81**: FD

- Eccentric, equatorial geodesics

  Warburton & Barack (2011) **PRD 83**: FD

  Thornburg & Wardell (2017) **PRD 95**: TD

- Circular, inclined geodesics

  Warburton (2015) **PRD 91**: FD

- Eccentric, inclined geodesics

  This work (2017): FD

Scalar self-force (SSF) as a toy model

SSF on Schwarzschild

- Circular geodesics

  Burko (2000) **PRL 84**: Freq. Domain (FD)

  Diaz-Rivera et al. (2004) **PRD 70**: FD

  Vega & Detweiler (2008) **PRD 77**: Time Domain (TD)

  Vega et al. (2009) **PRD 80**: TD

  Dolan & Barack (2011) **PRD 83**: TD

- Eccentric geodesics

  Haas (2007) **PRD 75**: TD

  Canizares et al. (2010) **PRD 82**: TD

  Diener et al. (2012) **PRL 102**: Effective source, TD

  Wardell et al. (2014) **PRD 89**: TD

SSF on Kerr

- Circular, equatorial geodesics

  Warburton & Barack (2010) **PRD 81**: FD

- Eccentric, equatorial geodesics

  Warburton & Barack (2011) **PRD 83**: FD

  Thornburg & Wardell (2017) **PRD 95**: TD

- Circular, inclined geodesics

  Warburton (2015) **PRD 91**: FD

- Eccentric, inclined geodesics

  This work (2017): FD

Scalar self-force (SSF) as a toy model

SSF on Schwarzschild

- Circular geodesics

  Burko (2000) **PRL 84**: Freq. Domain (FD)

  Diaz-Rivera et al. (2004) **PRD 70**: FD

  Vega & Detweiler (2008) **PRD 77**: Time Domain (TD)

  Vega et al. (2009) **PRD 80**: TD

  Dolan & Barack (2011) **PRD 83**: TD

- Eccentric geodesics

  Haas (2007) **PRD 75**: TD

  Canizares et al. (2010) **PRD 82**: TD

  Diener et al. (2012) **PRL 102**: Effective source, TD

  Wardell et al. (2014) **PRD 89**: TD

SSF on Kerr

- Circular, equatorial geodesics

  Warburton & Barack (2010) **PRD 81**: FD

- Eccentric, equatorial geodesics

  Warburton & Barack (2011) **PRD 83**: FD

  Thornburg & Wardell (2017) **PRD 95**: TD

- Circular, inclined geodesics

  Warburton (2015) **PRD 91**: FD

- Eccentric, inclined geodesics

  This work (2017): FD

Scalar self-force (SSF) as a toy model

SSF on Schwarzschild

- Circular geodesics

  Burko (2000) **PRL 84**: Freq. Domain (FD)

  Diaz-Rivera et al. (2004) **PRD 70**: FD

  Vega & Detweiler (2008) **PRD 77**: Time Domain (TD)

  Vega et al. (2009) **PRD 80**: TD

  Dolan & Barack (2011) **PRD 83**: TD

- Eccentric geodesics

  Haas (2007) **PRD 75**: TD

  Canizares et al. (2010) **PRD 82**: TD

  Diener et al. (2012) **PRL 102**: Effective source, TD

  Wardell et al. (2014) **PRD 89**: TD

SSF on Kerr

- Circular, equatorial geodesics

  Warburton & Barack (2010) **PRD 81**: FD

- Eccentric, equatorial geodesics

  Warburton & Barack (2011) **PRD 83**: FD

  Thornburg & Wardell (2017) **PRD 95**: TD

- Circular, inclined geodesics

  Warburton (2015) **PRD 91**: FD

- Eccentric, inclined geodesics

  This work (2017): FD

Scalar self-force (SSF) as a toy model

SSF on Schwarzschild

- Circular geodesics

  Burko (2000) **PRL 84**: Freq. Domain (FD)

  Diaz-Rivera et al. (2004) **PRD 70**: FD

  Vega & Detweiler (2008) **PRD 77**: Time Domain (TD)

  Vega et al. (2009) **PRD 80**: TD

  Dolan & Barack (2011) **PRD 83**: TD

- Eccentric geodesics

  Haas (2007) **PRD 75**: TD

  Canizares et al. (2010) **PRD 82**: TD

  Diener et al. (2012) **PRL 102**: Effective source, TD

  Wardell et al. (2014) **PRD 89**: TD

SSF on Kerr

- Circular, equatorial geodesics

  Warburton & Barack (2010) **PRD 81**: FD

- Eccentric, equatorial geodesics

  Warburton & Barack (2011) **PRD 83**: FD

  Thornburg & Wardell (2017) **PRD 95**: TD

- Circular, inclined geodesics

  Warburton (2015) **PRD 91**: FD

- Eccentric, inclined geodesics

  This work (2017): FD

Scalar self-force (SSF) as a toy model

SSF on Schwarzschild

- Circular geodesics

  Burko (2000) **PRL 84**: Freq. Domain (FD)

  Diaz-Rivera et al. (2004) **PRD 70**: FD

  Vega & Detweiler (2008) **PRD 77**: Time Domain (TD)

  Vega et al. (2009) **PRD 80**: TD

  Dolan & Barack (2011) **PRD 83**: TD

- Eccentric geodesics

  Haas (2007) **PRD 75**: TD

  Canizares et al. (2010) **PRD 82**: TD

  Diener et al. (2012) **PRL 102**: Effective source, TD

  Wardell et al. (2014) **PRD 89**: TD

SSF on Kerr

- Circular, equatorial geodesics

  Warburton & Barack (2010) **PRD 81**: FD

- Eccentric, equatorial geodesics

  Warburton & Barack (2011) **PRD 83**: FD

  Thornburg & Wardell (2017) **PRD 95**: TD

- Circular, inclined geodesics

  Warburton (2015) **PRD 91**: FD

- Eccentric, inclined geodesics

  This work (2017): FD

Scalar Self-Force (SSF)

$$F^{\alpha}_{\rm SSF} \equiv q\nabla^{\alpha}\Phi^{\rm R} = u^{\beta}\nabla_{\beta}\left(\mu u^{\alpha}\right)$$

Solving for the $F^{\alpha}_{\rm SSF}$

(1) Find the background geodesic motion on Kerr of scalar-charged particle
$\Longrightarrow$ source term

(2) Solve for the field using Klein-Gordon scalar wave-equation
$\Longrightarrow$ physical, *retarded* field $\Phi^{\rm ret}$

(3) Example - Detweiler-Whiting decomposition: $\Phi^{\rm ret} = \Phi^{\rm R} + \Phi^{\rm S}$
[Detweiler & Whiting (2003) **PRD 67**]
$\Longrightarrow$ regularization scheme

Mode-sum regularization [Barack & Ori (2003) **PRL 90**]

$$F^{\rm self}_{\alpha} = \sum_{\bar{l}=0}^{\infty}\left[F^{\bar{l}}_{\alpha} - F^{\bar{l}(\rm S)}_{\alpha}\right]$$

$$= \sum_{\bar{l}=0}^{\infty}\left[F^{\bar{l}}_{\alpha} - A_{\alpha}(\bar{l}+1/2) - B_{\alpha} - \mathcal{O}((\bar{l}+1/2)^{-1})\right]$$

- Improved convergence for equatorial orbits [Heffernan, Ottewill & Wardell (2014) **PRD 89**]

Scalar Self-Force (SSF)

$$F^{\alpha}_{\mathrm{SSF}} \equiv q\nabla^{\alpha}\Phi^{\mathrm{R}} = u^{\beta}\nabla_{\beta}\left(\mu u^{\alpha}\right)$$

Solving for the $F^{\alpha}_{\mathrm{SSF}}$

(1) Find the background geodesic motion on Kerr of scalar-charged particle
$\implies$ source term

(2) Solve for the field using Klein-Gordon scalar wave-equation
$\implies$ physical, *retarded* field Φ^{ret}

(3) Example - Detweiler-Whiting decomposition: $\Phi^{\mathrm{ret}} = \Phi^{\mathrm{R}} + \Phi^{\mathrm{S}}$
[Detweiler & Whiting (2003) **PRD 67**]
$\implies$ regularization scheme

Mode-sum regularization [Barack & Ori (2003) **PRL 90**]

$$F^{\mathrm{self}}_{\alpha} = \sum_{\bar{l}=0}^{\infty}\left[F^{\bar{l}}_{\alpha} - F^{\bar{l}(\mathrm{S})}_{\alpha}\right]$$

$$= \sum_{\bar{l}=0}^{\infty}\left[F^{\bar{l}}_{\alpha} - A_{\alpha}(\bar{l}+1/2) - B_{\alpha} - \mathcal{O}((\bar{l}+1/2)^{-1})\right]$$

- Improved convergence for equatorial orbits [Heffernan, Ottewill & Wardell (2014) **PRD 89**]

Scalar Self-Force (SSF)

$$F^{\alpha}_{\rm SSF} \equiv q\nabla^{\alpha}\Phi^{\rm R} = u^{\beta}\nabla_{\beta}\left(\mu u^{\alpha}\right)$$

Solving for the $F^{\alpha}_{\rm SSF}$

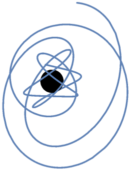

(1) Find the background geodesic motion on Kerr of scalar-charged particle
$\Longrightarrow$ source term

(2) Solve for the field using Klein-Gordon scalar wave-equation
$\Longrightarrow$ physical, *retarded* field $\Phi^{\rm ret}$

(3) Example - Detweiler-Whiting decomposition: $\Phi^{\rm ret} = \Phi^{\rm R} + \Phi^{\rm S}$
[Detweiler & Whiting (2003) **PRD 67**]
$\Longrightarrow$ regularization scheme

Mode-sum regularization [Barack & Ori (2003) **PRL 90**]

$$F^{\rm self}_{\alpha} = \sum_{\bar{l}=0}^{\infty}\left[F^{\bar{l}}_{\alpha} - F^{\bar{l}(\rm S)}_{\alpha}\right]$$
$$= \sum_{\bar{l}=0}^{\infty}\left[F^{\bar{l}}_{\alpha} - A_{\alpha}(\bar{l}+1/2) - B_{\alpha} - \mathcal{O}((\bar{l}+1/2)^{-1})\right]$$

- Improved convergence for equatorial orbits [Heffernan, Ottewill & Wardell (2014) **PRD 89**]

Scalar Self-Force (SSF)

$$F^\alpha_{\mathrm{SSF}} \equiv q\nabla^\alpha\Phi^{\mathrm{R}} = u^\beta\nabla_\beta\left(\mu u^\alpha\right)$$

Solving for the F^α_{SSF}

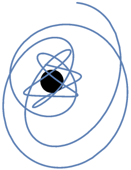

(1) Find the background geodesic motion on Kerr of scalar-charged particle
$\Longrightarrow$ source term

(2) Solve for the field using Klein-Gordon scalar wave-equation
$\Longrightarrow$ physical, *retarded* field Φ^{ret}

(3) Example - Detweiler-Whiting decomposition: $\Phi^{\mathrm{ret}} = \Phi^{\mathrm{R}} + \Phi^{\mathrm{S}}$
[Detweiler & Whiting (2003) **PRD 67**]
$\Longrightarrow$ regularization scheme

Mode-sum regularization [Barack & Ori (2003) **PRL 90**]

$$F^{\mathrm{self}}_\alpha = \sum_{\bar{l}=0}^{\infty}\left[F^{\bar{l}}_\alpha - F^{\bar{l}(\mathrm{S})}_\alpha\right]$$

$$= \sum_{\bar{l}=0}^{\infty}\left[F^{\bar{l}}_\alpha - A_\alpha(\bar{l}+1/2) - B_\alpha - \mathcal{O}((\bar{l}+1/2)^{-1})\right]$$

- Improved convergence for equatorial orbits [Heffernan, Ottewill & Wardell (2014) **PRD 89**]

Scalar Self-Force (SSF)

$$F^{\alpha}_{\mathrm{SSF}} \equiv q\nabla^{\alpha}\Phi^{\mathrm{R}} = u^{\beta}\nabla_{\beta}\left(\mu u^{\alpha}\right)$$

Solving for the $F^{\alpha}_{\mathrm{SSF}}$

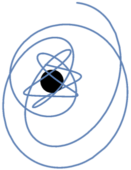

(1) Find the background geodesic motion on Kerr of scalar-charged particle
$\Longrightarrow$ source term

(2) Solve for the field using Klein-Gordon scalar wave-equation
$\Longrightarrow$ physical, *retarded* field Φ^{ret}

(3) Example - Detweiler-Whiting decomposition: $\Phi^{\mathrm{ret}} = \Phi^{\mathrm{R}} + \Phi^{\mathrm{S}}$
[Detweiler & Whiting (2003) **PRD 67**]
$\Longrightarrow$ regularization scheme

Mode-sum regularization [Barack & Ori (2003) **PRL 90**]

$$F_{\alpha}^{\mathrm{self}} = \sum_{\bar{l}=0}^{\infty}\left[F_{\alpha}^{\bar{l}} - F_{\alpha}^{\bar{l}(\mathrm{S})}\right]$$

$$= \sum_{\bar{l}=0}^{\infty}\left[F_{\alpha}^{\bar{l}} - A_{\alpha}(\bar{l}+1/2) - B_{\alpha} - \mathcal{O}((\bar{l}+1/2)^{-1})\right]$$

- Improved convergence for equatorial orbits [Heffernan, Ottewill & Wardell (2014) **PRD 89**]

Scalar Self-Force (SSF)

$$F^{\alpha}_{\mathrm{SSF}} \equiv q\nabla^{\alpha}\Phi^{\mathrm{R}} = u^{\beta}\nabla_{\beta}\left(\mu u^{\alpha}\right)$$

Solving for the $F^{\alpha}_{\mathrm{SSF}}$

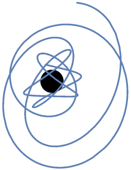

(1) Find the background geodesic motion on Kerr of scalar-charged particle
$\Longrightarrow$ source term

(2) Solve for the field using Klein-Gordon scalar wave-equation
$\Longrightarrow$ physical, *retarded* field Φ^{ret}

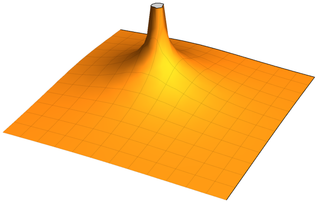

(3) Example - Detweiler-Whiting decomposition: $\Phi^{\mathrm{ret}} = \Phi^{\mathrm{R}} + \Phi^{\mathrm{S}}$
[Detweiler & Whiting (2003) **PRD 67**]
$\Longrightarrow$ regularization scheme

Mode-sum regularization [Barack & Ori (2003) **PRL 90**]

$$F^{\mathrm{self}}_{\alpha} = \sum_{\bar{l}=0}^{\infty}\left[F^{\bar{l}}_{\alpha} - F^{\bar{l}(\mathrm{S})}_{\alpha}\right]$$

$$= \sum_{\bar{l}=0}^{\infty}\left[F^{\bar{l}}_{\alpha} - A_{\alpha}(\bar{l}+1/2) - B_{\alpha} - \mathcal{O}((\bar{l}+1/2)^{-1})\right]$$

- Improved convergence for equatorial orbits [Heffernan, Ottewill & Wardell (2014) **PRD 89**]

Scalar Self-Force (SSF)

$$F^{\alpha}_{\text{SSF}} \equiv q\nabla^{\alpha}\Phi^{\text{R}} = u^{\beta}\nabla_{\beta}\left(\mu u^{\alpha}\right)$$

Solving for the F^{α}_{SSF}

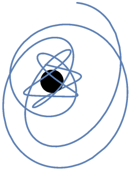

(1) Find the background geodesic motion on Kerr of scalar-charged particle
$\Longrightarrow$ source term

(2) Solve for the field using Klein-Gordon scalar wave-equation
$\Longrightarrow$ physical, *retarded* field Φ^{ret}

(3) Example - Detweiler-Whiting decomposition: $\Phi^{\text{ret}} = \Phi^{\text{R}} + \Phi^{\text{S}}$
[Detweiler & Whiting (2003) **PRD 67**]
$\Longrightarrow$ regularization scheme

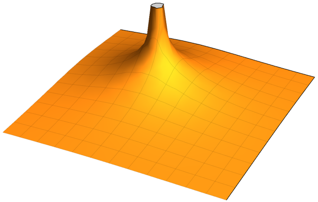

Mode-sum regularization [Barack & Ori (2003) **PRL 90**]

$$F^{\text{self}}_{\alpha} = \sum_{\bar{l}=0}^{\infty}\left[F^{\bar{l}}_{\alpha} - F^{\bar{l}(\text{S})}_{\alpha}\right]$$

$$= \sum_{\bar{l}=0}^{\infty}\left[F^{\bar{l}}_{\alpha} - A_{\alpha}(\bar{l}+1/2) - B_{\alpha} - \mathcal{O}((\bar{l}+1/2)^{-1})\right]$$

- Improved convergence for equatorial orbits [Heffernan, Ottewill & Wardell (2014) **PRD 89**]

Scalar Self-Force (SSF)

$$F^{\alpha}_{\mathrm{SSF}} \equiv q\nabla^{\alpha}\Phi^{\mathrm{R}} = u^{\beta}\nabla_{\beta}\left(\mu u^{\alpha}\right)$$

Solving for the $F^{\alpha}_{\mathrm{SSF}}$

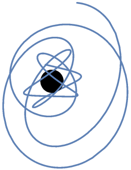

(1) Find the background geodesic motion on Kerr of scalar-charged particle
$\Longrightarrow$ source term

(2) Solve for the field using Klein-Gordon scalar wave-equation
$\Longrightarrow$ physical, *retarded* field Φ^{ret}

(3) Example - Detweiler-Whiting decomposition: $\Phi^{\mathrm{ret}} = \Phi^{\mathrm{R}} + \Phi^{\mathrm{S}}$
[Detweiler & Whiting (2003) **PRD 67**]
$\Longrightarrow$ regularization scheme

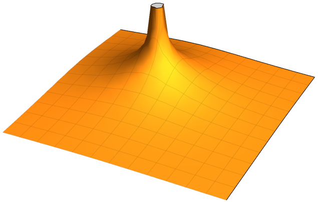

Mode-sum regularization [Barack & Ori (2003) **PRL 90**]

$$F^{\mathrm{self}}_{\alpha} = \sum_{\bar{l}=0}^{\infty}\left[F^{\bar{l}}_{\alpha} - F^{\bar{l}(\mathrm{S})}_{\alpha}\right]$$

$$= \sum_{\bar{l}=0}^{\infty}\left[F^{\bar{l}}_{\alpha} - A_{\alpha}(\bar{l}+1/2) - B_{\alpha} - \mathcal{O}((\bar{l}+1/2)^{-1})\right]$$

- Improved convergence for equatorial orbits [Heffernan, Ottewill & Wardell (2014) **PRD 89**]

Scalar Self-Force (SSF)

$$F^{\alpha}_{\mathrm{SSF}} \equiv q\nabla^{\alpha}\Phi^{\mathrm{R}} = u^{\beta}\nabla_{\beta}\left(\mu u^{\alpha}\right)$$

Solving for the $F^{\alpha}_{\mathrm{SSF}}$

(1) Find the background geodesic motion on Kerr of scalar-charged particle
$\Longrightarrow$ source term

(2) Solve for the field using Klein-Gordon scalar wave-equation
$\Longrightarrow$ physical, *retarded* field Φ^{ret}

(3) Example - Detweiler-Whiting decomposition: $\Phi^{\mathrm{ret}} = \Phi^{\mathrm{R}} + \Phi^{\mathrm{S}}$
[Detweiler & Whiting (2003) **PRD 67**]
$\Longrightarrow$ regularization scheme

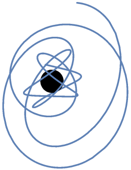

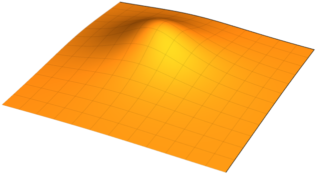

Mode-sum regularization [Barack & Ori (2003) **PRL 90**]

$$F^{\mathrm{self}}_{\alpha} = \sum_{\bar{l}=0}^{\infty}\left[F^{\bar{l}}_{\alpha} - F^{\bar{l}(\mathrm{S})}_{\alpha}\right]$$

$$= \sum_{\bar{l}=0}^{\infty}\left[F^{\bar{l}}_{\alpha} - A_{\alpha}(\bar{l}+1/2) - B_{\alpha} - \mathcal{O}((\bar{l}+1/2)^{-1})\right]$$

- Improved convergence for equatorial orbits [Heffernan, Ottewill & Wardell (2014) **PRD 89**]

Scalar Self-Force (SSF)

$$F^{\alpha}_{\mathrm{SSF}} \equiv q\nabla^{\alpha}\Phi^{\mathrm{R}} = u^{\beta}\nabla_{\beta}\left(\mu u^{\alpha}\right)$$

Solving for the $F^{\alpha}_{\mathrm{SSF}}$

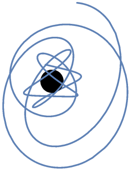

(1) Find the background geodesic motion on Kerr of scalar-charged particle
$\Longrightarrow$ source term

(2) Solve for the field using Klein-Gordon scalar wave-equation
$\Longrightarrow$ physical, *retarded* field Φ^{ret}

(3) Example - Detweiler-Whiting decomposition: $\Phi^{\mathrm{ret}} = \Phi^{\mathrm{R}} + \Phi^{\mathrm{S}}$
[Detweiler & Whiting (2003) **PRD 67**]
$\Longrightarrow$ regularization scheme

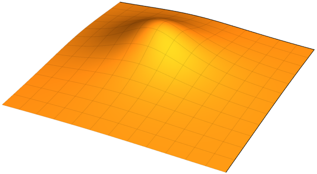

Mode-sum regularization [Barack & Ori (2003) **PRL 90**]

$$F^{\mathrm{self}}_{\alpha} = \sum_{\bar{l}=0}^{\infty}\left[F^{\bar{l}(\mathrm{ret})}_{\alpha} - F^{\bar{l}(\mathrm{S})}_{\alpha}\right]$$

$$= \sum_{\bar{l}=0}^{\infty}\left[F^{\bar{l}(\mathrm{ret})}_{\alpha} - A_{\alpha}(\bar{l}+1/2) - B_{\alpha} - \mathcal{O}((\bar{l}+1/2)^{-1})\right]$$

- Improved convergence for equatorial orbits [Heffernan, Ottewill & Wardell (2014) **PRD 89**]

Scalar Self-Force (SSF)

$$F^\alpha_{\text{SSF}} \equiv q\nabla^\alpha \Phi^{\text{R}} = u^\beta \nabla_\beta \left(\mu u^\alpha\right)$$

Solving for the F^α_{SSF}

(1) Find the background geodesic motion on Kerr of scalar-charged particle
$\implies$ source term

(2) Solve for the field using Klein-Gordon scalar wave-equation
$\implies$ physical, *retarded* field Φ^{ret}

(3) Example - Detweiler-Whiting decomposition: $\Phi^{\text{ret}} = \Phi^{\text{R}} + \Phi^{\text{S}}$
[Detweiler & Whiting (2003) **PRD 67**]
$\implies$ regularization scheme

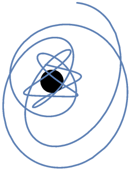

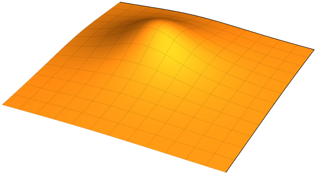

Mode-sum regularization [Barack & Ori (2003) **PRL 90**]

$$F^{\text{self}}_\alpha = \sum_{\bar{l}=0}^{\infty} \left[F^{\bar{l}(\text{cons})}_\alpha - F^{\bar{l}(\text{S})}_\alpha\right]$$

$$= \sum_{\bar{l}=0}^{\infty} \left[F^{\bar{l}(\text{cons})}_\alpha - A_\alpha(\bar{l}+1/2) - B_\alpha - \mathcal{O}((\bar{l}+1/2)^{-1})\right]$$

- Improved convergence for equatorial orbits [Heffernan, Ottewill & Wardell (2014) **PRD 89**]

Scalar Self-Force (SSF)

$$F^{\alpha}_{\mathrm{SSF}} \equiv q\nabla^{\alpha}\Phi^{\mathrm{R}} = u^{\beta}\nabla_{\beta}\left(\mu u^{\alpha}\right)$$

Solving for the $F^{\alpha}_{\mathrm{SSF}}$

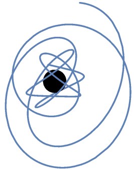

(1) Find the background geodesic motion on Kerr of scalar-charged particle
$\Longrightarrow$ source term

(2) Solve for the field using Klein-Gordon scalar wave-equation
$\Longrightarrow$ physical, *retarded* field Φ^{ret}

(3) Example - Detweiler-Whiting decomposition: $\Phi^{\mathrm{ret}} = \Phi^{\mathrm{R}} + \Phi^{\mathrm{S}}$
[Detweiler & Whiting (2003) **PRD 67**]
$\Longrightarrow$ regularization scheme

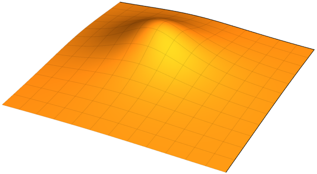

Mode-sum regularization [Barack & Ori (2003) **PRL 90**]

$$F^{\mathrm{self}}_{\alpha} = \sum_{\bar{l}=0}^{\infty}\left[F^{\bar{l}(\mathrm{cons})}_{\alpha} - F^{\bar{l}(\mathrm{S})}_{\alpha}\right]$$

$$= \sum_{\bar{l}=0}^{\infty}\left[F^{\bar{l}(\mathrm{cons})}_{\alpha} - A_{\alpha}(\bar{l}+1/2) - B_{\alpha} - \mathcal{O}((\bar{l}+1/2)^{-1})\right]$$

- Improved convergence for equatorial orbits [Heffernan, Ottewill & Wardell (2014) **PRD 89**]

Scalar field calculation

(1) Field equation due to scalar charge source $\Rightarrow$ spin-0 Teukolsky equations

$$\Box\Phi^{\mathrm{ret}} = -4\pi\sigma$$

(2) Calculate coupling of spheroidal harmonics with spherical harmonics

$$S_{lm}(-a^2\omega^2;\theta)e^{im\varphi} = \sum_{\bar{l}=m}^{\infty} b_{lm}^{\bar{l}}(-a^2\omega^2)Y_{\bar{l}m}(\theta,\varphi)$$

(3) Transform radial Teukolsky functions to Generalized Sasaki-Nakamura functions

$$\hat{R}_{lmkn}^{\mathrm{up/in}} \to \hat{X}_{lmkn}^{\pm} \qquad \Longrightarrow \qquad \left[\frac{d^2}{dr_*^2} + U_{lmkn}(r)\right]\tilde{X}_{lmkn}(r) = \tilde{\sigma}_{lmkn}(r) \qquad \& \qquad \hat{X}^{\pm} \sim \begin{cases} e^{i\omega r_*} & r_* \to -\infty \\ e^{-i\gamma r_*} & r_* \to \infty \end{cases}$$

(4) Compute homogeneous radial solutions $\hat{X}^{\pm}$ $\Rightarrow$ variation of parameters

$$\hat{C}^{\pm} = \frac{1}{W}\int_{r_{\min}}^{r_{\max}} \frac{\hat{X}^{\mp}(r)\tilde{\sigma}(r)(r^2+a^2)}{\Delta}\,dr$$

w/ method of extended homogeneous solutions
[Barack, Ori, & Sago (2008) **PRD 78**]

(5) Reconstruct TD solution

$$\tilde{X}_{lm}^{\pm}(t,r) = \sum_{kn} \begin{cases} C_{lmkn}^{+}\,\hat{X}_{lmkn}^{+}(r)\,e^{-i\omega_{mkn}t} & r \geq r_p(t) \\ C_{lmkn}^{-}\,\hat{X}_{lmkn}^{-}(r)\,e^{-i\omega_{mkn}t} & r \leq r_p(t) \end{cases}$$

Scalar field calculation

(1) Field equation due to scalar charge source $\Rightarrow$ spin-0 Teukolsky equations

$$\Box\Phi^{\text{ret}} = -4\pi\sigma$$

(2) Calculate coupling of spheroidal harmonics with spherical harmonics

$$S_{lm}(-a^2\omega^2;\theta)e^{im\varphi} = \sum_{\bar{l}=m}^{\infty} b_{lm}^{\bar{l}}(-a^2\omega^2)Y_{\bar{l}m}(\theta,\varphi)$$

(3) Transform radial Teukolsky functions to Generalized Sasaki-Nakamura functions

$$\hat{R}_{lmkn}^{\text{up/in}} \to \hat{X}_{lmkn}^{\pm} \quad \Longrightarrow \quad \left[\frac{d^2}{dr_*^2} + U_{lmkn}(r)\right]\tilde{X}_{lmkn}(r) = \tilde{\sigma}_{lmkn}(r) \quad \& \quad \hat{X}^{\pm} \sim \begin{cases} e^{i\omega r_*} & r_* \to -\infty \\ e^{-i\gamma r_*} & r_* \to \infty \end{cases}$$

(4) Compute homogeneous radial solutions $\hat{X}^{\pm} \Rightarrow$ variation of parameters

$$\hat{C}^{\pm} = \frac{1}{W}\int_{r_{\text{min}}}^{r_{\text{max}}} \frac{\hat{X}^{\mp}(r)\tilde{\sigma}(r)(r^2+a^2)}{\Delta}dr$$

w/ method of extended homogeneous solutions
[Barack, Ori, & Sago (2008) **PRD 78**]

(5) Reconstruct TD solution

$$\tilde{X}_{lm}^{\pm}(t,r) = \sum_{kn}\begin{cases} C_{lmkn}^{+}\,\hat{X}_{lmkn}^{+}(r)\,e^{-i\omega_{mkn}t} & r \geq r_p(t) \\ C_{lmkn}^{-}\,\hat{X}_{lmkn}^{-}(r)\,e^{-i\omega_{mkn}t} & r \leq r_p(t) \end{cases}$$

Scalar field calculation

(1) Field equation due to scalar charge source ⇒ spin-0 Teukolsky equations

$$\Box\Phi^{\mathrm{ret}} = -4\pi\sigma \qquad \Longrightarrow \qquad \Phi^{\mathrm{ret}} = \sum_{lmkn} R_{lmkn}(r) S_{lm}(-a^2\omega_{mkn}^2;\theta) e^{i(m\varphi - \omega_{mkn} t)}$$

(2) Calculate coupling of spheroidal harmonics with spherical harmonics

$$S_{lm}(-a^2\omega^2;\theta)e^{im\varphi} = \sum_{\bar{l}=m}^{\infty} b_{lm}^{\bar{l}}(-a^2\omega^2) Y_{\bar{l}m}(\theta,\varphi)$$

(3) Transform radial Teukolsky functions to Generalized Sasaki-Nakamura functions

$$\hat{R}_{lmkn}^{\mathrm{up/in}} \to \hat{X}_{lmkn}^{\pm} \qquad \Longrightarrow \qquad \left[\frac{d^2}{dr_*^2} + U_{lmkn}(r)\right]\tilde{X}_{lmkn}(r) = \tilde{\sigma}_{lmkn}(r) \qquad \& \qquad \hat{X}^{\pm} \sim \begin{cases} e^{i\omega r_*} & r_* \to -\infty \\ e^{-i\gamma r_*} & r_* \to \infty \end{cases}$$

(4) Compute homogeneous radial solutions $\hat{X}^{\pm}$ ⇒ variation of parameters

$$\hat{C}^{\pm} = \frac{1}{W}\int_{r_{\min}}^{r_{\max}} \frac{\hat{X}^{\mp}(r)\tilde{\sigma}(r)(r^2+a^2)}{\Delta} dr$$

w/ method of extended homogeneous solutions
[Barack, Ori, & Sago (2008) **PRD 78**]

(5) Reconstruct TD solution

$$\tilde{X}_{lm}^{\pm}(t,r) = \sum_{kn} \begin{cases} C_{lmkn}^{+}\,\hat{X}_{lmkn}^{+}(r)\,e^{-i\omega_{mkn}t} & r \geq r_p(t) \\ C_{lmkn}^{-}\,\hat{X}_{lmkn}^{-}(r)\,e^{-i\omega_{mkn}t} & r \leq r_p(t) \end{cases}$$

Scalar field calculation

(1) Field equation due to scalar charge source ⇒ spin-0 Teukolsky equations

$$\Box\Phi^{\text{ret}} = -4\pi\sigma \qquad \Longrightarrow \qquad \Phi^{\text{ret}} = \sum_{lmkn} R_{lmkn}(r) S_{lm}(-a^2\omega_{mkn}^2;\theta) e^{i(m\varphi - \omega_{mkn}t)}$$

(2) Calculate coupling of spheroidal harmonics with spherical harmonics

$$S_{lm}(-a^2\omega^2;\theta)e^{im\varphi} = \sum_{\bar{l}=m}^{\infty} b_{lm}^{\bar{l}}(-a^2\omega^2) Y_{\bar{l}m}(\theta,\varphi)$$

(3) Transform radial Teukolsky functions to Generalized Sasaki-Nakamura functions

$$\hat{R}_{lmkn}^{\text{up/in}} \to \hat{X}_{lmkn}^{\pm} \qquad \Longrightarrow \qquad \left[\frac{d^2}{dr_*^2} + U_{lmkn}(r)\right]\tilde{X}_{lmkn}(r) = \tilde{\sigma}_{lmkn}(r) \qquad \& \qquad \hat{X}^{\pm} \sim \begin{cases} e^{i\omega r_*} & r_* \to -\infty \\ e^{-i\gamma r_*} & r_* \to \infty \end{cases}$$

(4) Compute homogeneous radial solutions $\hat{X}^{\pm}$ ⇒ variation of parameters

$$\hat{C}^{\pm} = \frac{1}{W}\int_{r_{\min}}^{r_{\max}} \frac{\hat{X}^{\mp}(r)\tilde{\sigma}(r)(r^2+a^2)}{\Delta} dr$$

w/ method of extended homogeneous solutions
[Barack, Ori, & Sago (2008) **PRD 78**]

(5) Reconstruct TD solution

$$\tilde{X}_{lm}^{\pm}(t,r) = \sum_{kn} \begin{cases} C_{lmkn}^{+}\,\hat{X}_{lmkn}^{+}(r)\,e^{-i\omega_{mkn}t} & r \geq r_p(t) \\ C_{lmkn}^{-}\,\hat{X}_{lmkn}^{-}(r)\,e^{-i\omega_{mkn}t} & r \leq r_p(t) \end{cases}$$

Scalar field calculation

(1) Field equation due to scalar charge source ⇒ spin-0 Teukolsky equations

$$\Box\Phi^{\mathrm{ret}} = -4\pi\sigma \qquad \Longrightarrow \qquad \Phi^{\mathrm{ret}} = \sum_{lmkn} R_{lmkn}(r) S_{lm}(-a^2\omega_{mkn}^2;\theta) e^{i(m\varphi-\omega_{mkn}t)}$$

(2) Calculate coupling of spheroidal harmonics with spherical harmonics

$$S_{lm}(-a^2\omega^2;\theta)e^{im\varphi} = \sum_{\bar{l}=m}^{\infty} b_{lm}^{\bar{l}}(-a^2\omega^2) Y_{\bar{l}m}(\theta,\varphi) \qquad F_\alpha^{\mathrm{self}} = \sum_{\bar{l}=0}^{\infty}\left[F_\alpha^{\bar{l}(\mathrm{cons})} - F_\alpha^{\bar{l}(\mathrm{S})}\right]$$

(3) Transform radial Teukolsky functions to Generalized Sasaki-Nakamura functions

$$\hat{R}_{lmkn}^{\mathrm{up/in}} \to \hat{X}_{lmkn}^{\pm} \qquad \Longrightarrow \qquad \left[\frac{d^2}{dr_*^2} + U_{lmkn}(r)\right]\tilde{X}_{lmkn}(r) = \tilde{\sigma}_{lmkn}(r) \qquad \& \qquad \hat{X}^{\pm} \sim \begin{cases} e^{i\omega r_*} & r_* \to -\infty \\ e^{-i\gamma r_*} & r_* \to \infty \end{cases}$$

(4) Compute homogeneous radial solutions $\hat{X}^{\pm}$ ⇒ variation of parameters

$$\hat{C}^{\pm} = \frac{1}{W}\int_{r_{\min}}^{r_{\max}} \frac{\hat{X}^{\mp}(r)\tilde{\sigma}(r)(r^2+a^2)}{\Delta}\,dr$$

w/ method of extended homogeneous solutions
[Barack, Ori, & Sago (2008) **PRD 78**]

(5) Reconstruct TD solution

$$\tilde{X}_{lm}^{\pm}(t,r) = \sum_{kn}\begin{cases} C_{lmkn}^{+}\,\hat{X}_{lmkn}^{+}(r)\,e^{-i\omega_{mkn}t} & r \geq r_p(t) \\ C_{lmkn}^{-}\,\hat{X}_{lmkn}^{-}(r)\,e^{-i\omega_{mkn}t} & r \leq r_p(t) \end{cases}$$

Scalar field calculation

(1) Field equation due to scalar charge source $\Rightarrow$ spin-0 Teukolsky equations

$$\Box\Phi^{\text{ret}} = -4\pi\sigma \qquad \Longrightarrow \qquad \Phi^{\text{ret}} = \sum_{lmkn} R_{lmkn}(r) S_{lm}(-a^2\omega^2_{mkn};\theta) e^{i(m\varphi - \omega_{mkn}t)}$$

(2) Calculate coupling of spheroidal harmonics with spherical harmonics

$$S_{lm}(-a^2\omega^2;\theta)e^{im\varphi} = \sum_{\bar{l}=m}^{\infty} b^{\bar{l}}_{lm}(-a^2\omega^2) Y_{\bar{l}m}(\theta,\varphi) \qquad F^{\text{self}}_{\alpha} = \sum_{\bar{l}=0}^{\infty}\left[F^{\bar{l}(\text{cons})}_{\alpha} - F^{\bar{l}(\text{S})}_{\alpha}\right]$$

(3) Transform radial Teukolsky functions to Generalized Sasaki-Nakamura functions

$$\hat{R}^{\text{up/in}}_{lmkn} \to \hat{X}^{\pm}_{lmkn} \qquad \Longrightarrow \qquad \left[\frac{d^2}{dr_*^2} + U_{lmkn}(r)\right]\tilde{X}_{lmkn}(r) = \tilde{\sigma}_{lmkn}(r) \qquad \& \qquad \hat{X}^{\pm} \sim \begin{cases} e^{i\omega r_*} & r_* \to -\infty \\ e^{-i\gamma r_*} & r_* \to \infty \end{cases}$$

(4) Compute homogeneous radial solutions $\hat{X}^{\pm} \Rightarrow$ variation of parameters

$$\hat{C}^{\pm} = \frac{1}{W}\int_{r_{\min}}^{r_{\max}} \frac{\hat{X}^{\mp}(r)\tilde{\sigma}(r)(r^2+a^2)}{\Delta} dr$$

w/ method of extended homogeneous solutions
[Barack, Ori, & Sago (2008) **PRD 78**]

(5) Reconstruct TD solution

$$\tilde{X}^{\pm}_{lm}(t,r) = \sum_{kn}\begin{cases} C^{+}_{lmkn}\,\hat{X}^{+}_{lmkn}(r)\,e^{-i\omega_{mkn}t} & r \geq r_p(t) \\ C^{-}_{lmkn}\,\hat{X}^{-}_{lmkn}(r)\,e^{-i\omega_{mkn}t} & r \leq r_p(t) \end{cases}$$

Scalar field calculation

(1) Field equation due to scalar charge source $\Rightarrow$ spin-0 Teukolsky equations

$$\Box\Phi^{\text{ret}} = -4\pi\sigma \qquad \Longrightarrow \qquad \Phi^{\text{ret}} = \sum_{lmkn} R_{lmkn}(r) S_{lm}(-a^2\omega_{mkn}^2;\theta) e^{i(m\varphi - \omega_{mkn}t)}$$

(2) Calculate coupling of spheroidal harmonics with spherical harmonics

$$S_{lm}(-a^2\omega^2;\theta)e^{im\varphi} = \sum_{\bar{l}=m}^{\infty} b_{lm}^{\bar{l}}(-a^2\omega^2) Y_{\bar{l}m}(\theta,\varphi) \qquad F_\alpha^{\text{self}} = \sum_{\bar{l}=0}^{\infty}\left[F_\alpha^{\bar{l}(\text{cons})} - F_\alpha^{\bar{l}(\text{S})}\right]$$

(3) Transform radial Teukolsky functions to Generalized Sasaki-Nakamura functions

$$\hat{R}_{lmkn}^{\text{up/in}} \to \hat{X}_{lmkn}^{\pm} \qquad \Longrightarrow \qquad \left[\frac{d^2}{dr_*^2} + U_{lmkn}(r)\right]\tilde{X}_{lmkn}(r) = \tilde{\sigma}_{lmkn}(r) \qquad \& \qquad \hat{X}^{\pm} \sim \begin{cases} e^{i\omega r_*} & r_* \to -\infty \\ e^{-i\gamma r_*} & r_* \to \infty \end{cases}$$

(4) Compute homogeneous radial solutions $\hat{X}^{\pm}$ $\Rightarrow$ variation of parameters

$$\hat{C}^{\pm} = \frac{1}{W}\int_{r_{\min}}^{r_{\max}} \frac{\hat{X}^{\mp}(r)\tilde{\sigma}(r)(r^2+a^2)}{\Delta}dr$$

w/ method of extended homogeneous solutions
[Barack, Ori, & Sago (2008) **PRD 78**]

(5) Reconstruct TD solution

$$\tilde{X}_{lm}^{\pm}(t,r) = \sum_{kn}\begin{cases} C_{lmkn}^{+}\,\hat{X}_{lmkn}^{+}(r)\,e^{-i\omega_{mkn}t} & r \geq r_p(t) \\ C_{lmkn}^{-}\,\hat{X}_{lmkn}^{-}(r)\,e^{-i\omega_{mkn}t} & r \leq r_p(t) \end{cases}$$

Scalar field calculation

(1) Field equation due to scalar charge source ⇒ spin-0 Teukolsky equations

$$\Box\Phi^{\mathrm{ret}} = -4\pi\sigma \qquad \Longrightarrow \qquad \Phi^{\mathrm{ret}} = \sum_{lmkn} R_{lmkn}(r) S_{lm}(-a^2\omega_{mkn}^2;\theta) e^{i(m\varphi - \omega_{mkn}t)}$$

(2) Calculate coupling of spheroidal harmonics with spherical harmonics

$$S_{lm}(-a^2\omega^2;\theta)e^{im\varphi} = \sum_{\bar{l}=m}^{\infty} b_{lm}^{\bar{l}}(-a^2\omega^2) Y_{\bar{l}m}(\theta,\varphi) \qquad F_\alpha^{\mathrm{self}} = \sum_{\bar{l}=0}^{\infty}\left[F_\alpha^{\bar{l}(\mathrm{cons})} - F_\alpha^{\bar{l}(\mathrm{S})}\right]$$

(3) Transform radial Teukolsky functions to Generalized Sasaki-Nakamura functions

$$\hat{R}_{lmkn}^{\mathrm{up/in}} \to \hat{X}_{lmkn}^{\pm} \qquad \Longrightarrow \qquad \left[\frac{d^2}{dr_*^2} + U_{lmkn}(r)\right]\tilde{X}_{lmkn}(r) = \tilde{\sigma}_{lmkn}(r) \qquad \& \qquad \hat{X}^{\pm} \sim \begin{cases} e^{i\omega r_*} & r_* \to -\infty \\ e^{-i\gamma r_*} & r_* \to \infty \end{cases}$$

(4) Compute homogeneous radial solutions $\hat{X}^{\pm}$ ⇒ variation of parameters

$$\hat{C}^{\pm} = \frac{1}{W}\int_{r_{\min}}^{r_{\max}} \frac{\hat{X}^{\mp}(r)\tilde{\sigma}(r)(r^2+a^2)}{\Delta}\,dr$$

w/ method of extended homogeneous solutions
[Barack, Ori, & Sago (2008) **PRD 78**]

(5) Reconstruct TD solution

$$\tilde{X}_{lm}^{\pm}(t,r) = \sum_{kn}\begin{cases} C_{lmkn}^{+}\,\hat{X}_{lmkn}^{+}(r)\,e^{-i\omega_{mkn}t} & r \geq r_p(t) \\ C_{lmkn}^{-}\,\hat{X}_{lmkn}^{-}(r)\,e^{-i\omega_{mkn}t} & r \leq r_p(t) \end{cases}$$

Scalar field calculation

(1) Field equation due to scalar charge source $\Rightarrow$ spin-0 Teukolsky equations

$$\Box\Phi^{\mathrm{ret}} = -4\pi\sigma \qquad \Longrightarrow \qquad \Phi^{\mathrm{ret}} = \sum_{lmkn} R_{lmkn}(r) S_{lm}(-a^2\omega_{mkn}^2;\theta) e^{i(m\varphi - \omega_{mkn}t)}$$

(2) Calculate coupling of spheroidal harmonics with spherical harmonics

$$S_{lm}(-a^2\omega^2;\theta)e^{im\varphi} = \sum_{\bar{l}=m}^{\infty} b_{lm}^{\bar{l}}(-a^2\omega^2) Y_{\bar{l}m}(\theta,\varphi) \qquad F_\alpha^{\mathrm{self}} = \sum_{\bar{l}=0}^{\infty}\left[F_\alpha^{\bar{l}(\mathrm{cons})} - F_\alpha^{\bar{l}(\mathrm{S})}\right]$$

(3) Transform radial Teukolsky functions to Generalized Sasaki-Nakamura functions

$$\hat{R}_{lmkn}^{\mathrm{up/in}} \to \hat{X}_{lmkn}^{\pm} \qquad \Longrightarrow \qquad \left[\frac{d^2}{dr_*^2} + U_{lmkn}(r)\right]\tilde{X}_{lmkn}(r) = \tilde{\sigma}_{lmkn}(r) \qquad \& \qquad \hat{X}^{\pm} \sim \begin{cases} e^{i\omega r_*} & r_* \to -\infty \\ e^{-i\gamma r_*} & r_* \to \infty \end{cases}$$

(4) Compute homogeneous radial solutions $\hat{X}^{\pm}$ $\Rightarrow$ variation of parameters

$$\hat{C}^{\pm} = \frac{1}{W}\int_{r_{\min}}^{r_{\max}} \frac{\hat{X}^{\mp}(r)\tilde{\sigma}(r)(r^2+a^2)}{\Delta}\,dr$$

w/ method of extended homogeneous solutions
[Barack, Ori, & Sago (2008) **PRD 78**]

(5) Reconstruct TD solution

$$\tilde{X}_{lm}^{\pm}(t,r) = \sum_{kn}\begin{cases} C_{lmkn}^{+}\,\hat{X}_{lmkn}^{+}(r)\,e^{-i\omega_{mkn}t} & r \geq r_p(t) \\ C_{lmkn}^{-}\,\hat{X}_{lmkn}^{-}(r)\,e^{-i\omega_{mkn}t} & r \leq r_p(t) \end{cases}$$

SSF Code

- Mathematica-based code
  - Arbitrary numerical precision
  - Symbolic manipulation & output
- Formalisms
  - Frequency domain approach $\Rightarrow$ mode decomposition
  - Mano-Suzuki-Takasugi (MST) formalism
  - Spectral source integration (SSI)
- Implementation
  - Ran on campus cluster
  - Parallelized on $\{l, m\}$-mode basis

SSF Code

- MATHEMATICA-based code
  - Arbitrary numerical precision
  - Symbolic manipulation & output
- Formalisms
  - Frequency domain approach $\Rightarrow$ mode decomposition
  - Mano-Suzuki-Takasugi (MST) formalism
  - Spectral source integration (SSI)
- Implementation
  - Ran on campus cluster
  - Parallelized on $\{l, m\}$-mode basis

SSF Code

- MATHEMATICA-based code
  - Arbitrary numerical precision
  - Symbolic manipulation & output
- Formalisms
  - Frequency domain approach ⇒ mode decomposition
  - Mano-Suzuki-Takasugi (MST) formalism
  - Spectral source integration (SSI)
- Implementation
  - Ran on campus cluster
  - Parallelized on $\{l, m\}$-mode basis

SSF Code

- MATHEMATICA-based code
  - Arbitrary numerical precision
  - Symbolic manipulation & output
- Formalisms
  - Frequency domain approach $\Rightarrow$ mode decomposition
  - Mano-Suzuki-Takasugi (MST) formalism
  - Spectral source integration (SSI)
- Implementation
  - Ran on campus cluster
  - Parallelized on $\{l, m\}$-mode basis

SSF Code

- MATHEMATICA-based code
  - Arbitrary numerical precision
  - Symbolic manipulation & output
- Formalisms
  - Frequency domain approach $\Rightarrow$ mode decomposition
  - Mano-Suzuki-Takasugi (MST) formalism
  - Spectral source integration (SSI)
- Implementation
  - Ran on campus cluster
  - Parallelized on $\{l, m\}$-mode basis

SSF Code

- MATHEMATICA-based code
  - Arbitrary numerical precision
  - Symbolic manipulation & output
- Formalisms
  - Frequency domain approach $\Rightarrow$ mode decomposition
  - Mano-Suzuki-Takasugi (MST) formalism
  - Spectral source integration (SSI)
- Implementation
  - Ran on campus cluster
  - Parallelized on $\{l, m\}$-mode basis

SSF Code

- Mathematica-based code
  - Arbitrary numerical precision
  - Symbolic manipulation & output
- Formalisms
  - Frequency domain approach ⇒ mode decomposition
  - Mano-Suzuki-Takasugi (MST) formalism
  - Spectral source integration (SSI)
- Implementation
  - Ran on campus cluster
  - Parallelized on $\{l, m\}$-mode basis

SSF Code

- Mathematica-based code
  - Arbitrary numerical precision
  - Symbolic manipulation & output
- Formalisms
  - Frequency domain approach ⇒ mode decomposition
  - Mano-Suzuki-Takasugi (MST) formalism
  - Spectral source integration (SSI)
- Implementation
  - Ran on campus cluster
  - Parallelized on $\{l, m\}$-mode basis

SSF Code

- MATHEMATICA-based code
  - Arbitrary numerical precision
  - Symbolic manipulation & output
- Formalisms
  - Frequency domain approach $\Rightarrow$ mode decomposition
  - Mano-Suzuki-Takasugi (MST) formalism
  - Spectral source integration (SSI)
- Implementation
  - Ran on campus cluster
  - Parallelized on $\{l, m\}$-mode basis

SSF Code

- Mathematica-based code
  - Arbitrary numerical precision
  - Symbolic manipulation & output
- Formalisms
  - Frequency domain approach $\Rightarrow$ mode decomposition
  - Mano-Suzuki-Takasugi (MST) formalism
  - Spectral source integration (SSI)
- Implementation
  - Ran on campus cluster
  - Parallelized on $\{l, m\}$-mode basis

SSF Code

- MATHEMATICA-based code
  - Arbitrary numerical precision
  - Symbolic manipulation & output
- Formalisms
  - Frequency domain approach $\Rightarrow$ mode decomposition
  - Mano-Suzuki-Takasugi (MST) formalism
  - Spectral source integration (SSI)
- Implementation
  - Ran on campus cluster
  - Parallelized on $\{l, m\}$-mode basis

SSF Code

- Mathematica-based code
  - Arbitrary numerical precision
  - Symbolic manipulation & output
- Formalisms
  - Frequency domain approach $\Rightarrow$ mode decomposition
  - Mano-Suzuki-Takasugi (MST) formalism
  - Spectral source integration (SSI)
- Implementation
  - Ran on campus cluster
  - Parallelized on $\{l, m\}$-mode basis

Spectral source integration (SSI)

SSI on Schwarzschild [Hopper et al. (2015) **PRD 92**]

- Darwin's relativistic anomaly:

$$r_p = r_p(\psi) = \frac{pM}{1 + e\cos\chi}$$

- Integrands dependent on r_p periodic & C^∞

$$\int I\left[r_p(t)\right]\, dt$$

- Exponential convergence of Fourier sum $\Rightarrow$ calculations to 200 digits
- Number of points scales with number of digits of accuracy
- Useful for integrating orbits and source

Spectral source integration (SSI)

SSI on Schwarzschild [Hopper et al. (2015) **PRD 92**]

- Darwin's relativistic anomaly:

$$r_p = r_p(\psi) = \frac{pM}{1 + e\cos\chi}$$

- Integrands dependent on r_p periodic & C^∞

$$\int I\left[r_p(t)\right]\,dt$$

- Exponential convergence of Fourier sum $\Rightarrow$ calculations to 200 digits
- Number of points scales with number of digits of accuracy
- Useful for integrating orbits and source

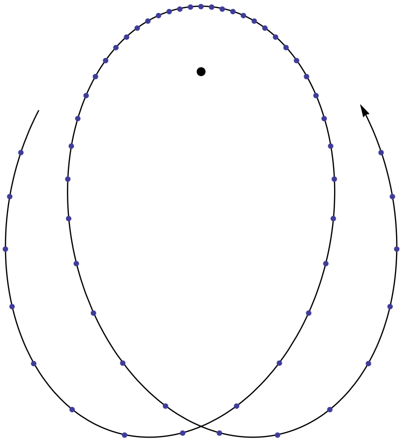

Spectral source integration (SSI)

SSI on Schwarzschild [Hopper et al. (2015) **PRD 92**]

- Darwin's relativistic anomaly:

$$r_p = r_p(\psi) = \frac{pM}{1 + e\cos\chi}$$

- Integrands dependent on r_p periodic & C^∞

$$\int I\left[r_p(t)\right]\, dt$$

- Exponential convergence of Fourier sum $\Rightarrow$ calculations to 200 digits
- Number of points scales with number of digits of accuracy
- Useful for integrating orbits and source

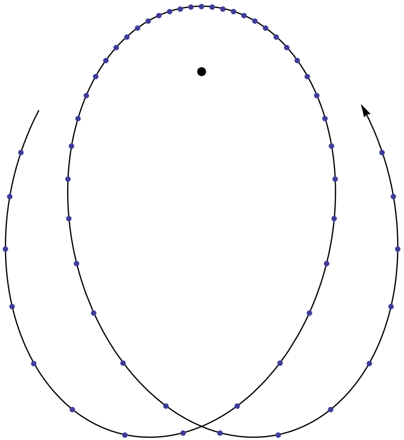

Spectral source integration (SSI)

SSI on Schwarzschild [Hopper et al. (2015) **PRD 92**]

- Darwin's relativistic anomaly:

$$r_p = r_p(\psi) = \frac{pM}{1 + e\cos\chi}$$

- Integrands dependent on r_p periodic & C^∞

$$\int I\left[r_p(t)\right]\, dt$$

- Exponential convergence of Fourier sum $\Rightarrow$ calculations to 200 digits
- Number of points scales with number of digits of accuracy
- Useful for integrating orbits and source

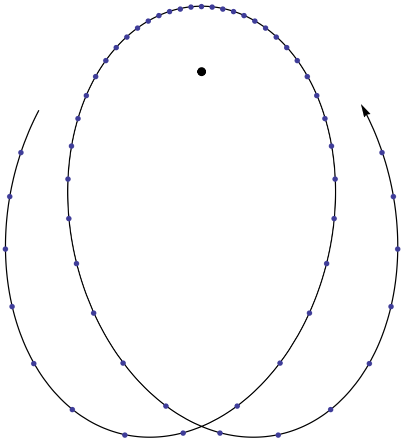

Spectral source integration (SSI)

SSI on Schwarzschild [Hopper et al. (2015) **PRD 92**]

- Darwin's relativistic anomaly:

$$r_p = r_p(\psi) = \frac{pM}{1 + e\cos\chi}$$

- Integrands dependent on r_p periodic & C^∞
  $\Rightarrow$ replaced by DFT w/ samples along orbit

$$\int I\left[r_p(t)\right]\, dt \qquad \Longrightarrow \qquad \sum_i I(\chi_i)$$

- Exponential convergence of Fourier sum $\Rightarrow$ calculations to 200 digits

- Number of points scales with number of digits of accuracy

- Useful for integrating orbits and source

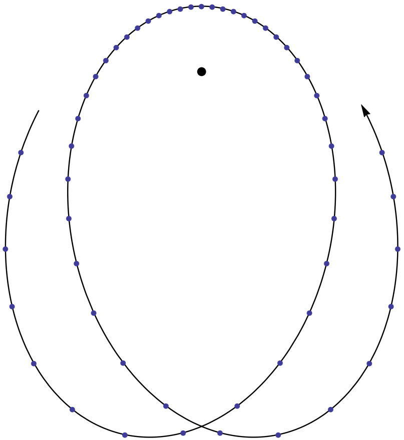

Spectral source integration (SSI)

SSI on Schwarzschild [Hopper et al. (2015) **PRD 92**]

- Darwin's relativistic anomaly:

$$r_p = r_p(\psi) = \frac{pM}{1 + e\cos\chi}$$

- Integrands dependent on r_p periodic & C^∞
  $\Rightarrow$ replaced by DFT w/ samples along orbit

$$\int I\left[r_p(t)\right]\, dt \qquad \Longrightarrow \qquad \sum_i I(\chi_i)$$

- Exponential convergence of Fourier sum $\Rightarrow$ calculations to 200 digits

- Number of points scales with number of digits of accuracy

- Useful for integrating orbits and source

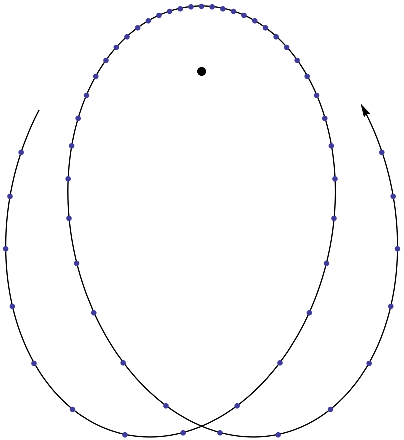

Spectral source integration (SSI)

SSI on Schwarzschild [Hopper et al. (2015) **PRD 92**]

- Darwin's relativistic anomaly:

$$r_p = r_p(\psi) = \frac{pM}{1 + e\cos\chi}$$

- Integrands dependent on r_p periodic & C^∞
  $\Rightarrow$ replaced by DFT w/ samples along orbit

$$\int I\left[r_p(t)\right]\, dt \qquad \Longrightarrow \qquad \sum_i I(\chi_i)$$

- Exponential convergence of Fourier sum $\Rightarrow$ calculations to 200 digits
- Number of points scales with number of digits of accuracy
- Useful for integrating orbits and source

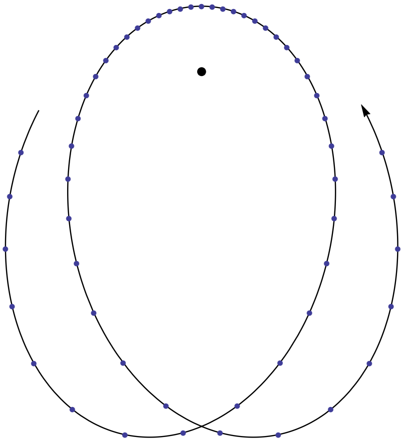

Spectral source integration (SSI)

SSI on Schwarzschild [Hopper et al. (2015) **PRD 92**]

- Darwin's relativistic anomaly:

$$r_p = r_p(\psi) = \frac{pM}{1 + e\cos\chi}$$

- Integrands dependent on r_p periodic & C^∞
  $\Rightarrow$ replaced by DFT w/ samples along orbit

$$\int I\left[r_p(t)\right]\, dt \qquad \Longrightarrow \qquad \sum_i I(\chi_i)$$

- Exponential convergence of Fourier sum $\Rightarrow$ calculations to 200 digits
- Number of points scales with number of digits of accuracy
- Useful for integrating orbits and source

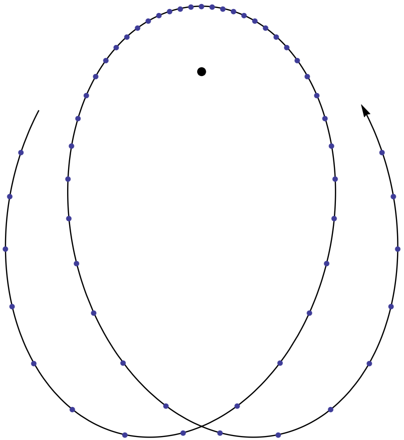

SSI on Kerr

Source integration on Kerr

$$\hat{C}^{\pm} = \frac{1}{W} \int_{r_{\min}}^{r_{\max}} \frac{\hat{X}^{\mp}(r)\tilde{\sigma}(r)(r^2 + a^2)}{\Delta} dr$$

- Mino time $\lambda \Rightarrow$ separate $\{r_p, \theta_p\}$ peridocity

$$r_p(\psi) = \frac{pM}{1 + e\cos\psi} \qquad \cos\theta_p(\chi) = \sqrt{z_-}\cos\chi$$

$$\hat{C}^{\pm} = \int d\psi \int d\chi \tilde{A}^{\pm}(\psi, \chi)$$

- Separate into 1D integrals (for $s = 0$)

$$\hat{C}^{\pm} = \int d\psi \tilde{F}_1^{\pm}(\psi) \int d\chi \tilde{F}_2(\chi) + \int d\psi \tilde{F}_3^{\pm}(\psi) \int d\chi \tilde{F}_4(\chi)$$

- Convert to discrete Fourier sums

$$\hat{C}^{\pm} = I_1^{\pm} I_2 + I_3^{\pm} I_4 \qquad \text{w/} \qquad I_1^{\pm} \sim \sum_{i=0}^{N_1 - 1} \tilde{F}_1^{\pm}(\psi_i)$$

- Numerical integration in 2D $\Rightarrow$ compute 4 1D Fourier sums

Computational efficiency of SSI on Kerr

- $a/M = 0.5$, $e = 0.5$, $p = 15$, $\iota = \pi/3$
- Calculate $C^{\pm}_{2222}$ mode

SSI on Kerr

Source integration on Kerr

$$\hat{C}^{\pm} = \frac{1}{W}\int_{r_{\min}}^{r_{\max}} \frac{\hat{X}^{\mp}(r)\tilde{\sigma}(r)(r^2+a^2)}{\Delta} dr$$

- Mino time $\lambda \Rightarrow$ separate $\{r_p, \theta_p\}$ peridocity

$$r_p(\psi) = \frac{pM}{1+e\cos\psi} \qquad \cos\theta_p(\chi) = \sqrt{z_-}\cos\chi$$

$$\hat{C}^{\pm} = \int d\psi \int d\chi \tilde{A}^{\pm}(\psi,\chi)$$

- Separate into 1D integrals (for $s=0$)

$$\hat{C}^{\pm} = \int d\psi \tilde{F}_1^{\pm}(\psi) \int d\chi \tilde{F}_2(\chi) + \int d\psi \tilde{F}_3^{\pm}(\psi) \int d\chi \tilde{F}_4(\chi)$$

- Convert to discrete Fourier sums

$$\hat{C}^{\pm} = I_1^{\pm} I_2 + I_3^{\pm} I_4 \qquad \text{w/} \qquad I_1^{\pm} \sim \sum_{i=0}^{N_1-1} \tilde{F}_1^{\pm}(\psi_i)$$

- Numerical integration in 2D $\Rightarrow$ compute 4 1D Fourier sums

Computational efficiency of SSI on Kerr

- $a/M = 0.5$, $e = 0.5$, $p = 15$, $\iota = \pi/3$
- Calculate $C_{2222}^{\pm}$ mode

SSI on Kerr

Source integration on Kerr

$$\hat{C}^{\pm} = \frac{1}{W}\int_{r_{\min}}^{r_{\max}} \frac{\hat{X}^{\mp}(r)\tilde{\sigma}(r)(r^2+a^2)}{\Delta}\,dr$$

- Mino time $\lambda \Rightarrow$ separate $\{r_p, \theta_p\}$ peridocity

$$r_p(\psi) = \frac{pM}{1+e\cos\psi} \qquad \cos\theta_p(\chi) = \sqrt{z_-}\cos\chi$$

$$\hat{C}^{\pm} = \int d\psi \int d\chi \tilde{A}^{\pm}(\psi,\chi)$$

- Separate into 1D integrals (for $s=0$)

$$\hat{C}^{\pm} = \int d\psi \tilde{F}_1^{\pm}(\psi)\int d\chi \tilde{F}_2(\chi) + \int d\psi \tilde{F}_3^{\pm}(\psi)\int d\chi \tilde{F}_4(\chi)$$

- Convert to discrete Fourier sums

$$\hat{C}^{\pm} = I_1^{\pm} I_2 + I_3^{\pm} I_4 \qquad \text{w/} \qquad I_1^{\pm} \sim \sum_{i=0}^{N_1-1} \tilde{F}_1^{\pm}(\psi_i)$$

- Numerical integration in 2D $\Rightarrow$ compute 4 1D Fourier sums

Computational efficiency of SSI on Kerr

- $a/M = 0.5$, $e = 0.5$, $p = 15$, $\iota = \pi/3$
- Calculate $C_{2222}^{\pm}$ mode

SSI on Kerr

Source integration on Kerr

$$\hat{C}^{\pm} = \frac{1}{W}\int_{r_{\min}}^{r_{\max}} \frac{\hat{X}^{\mp}(r)\tilde{\sigma}(r)(r^2+a^2)}{\Delta}dr$$

- Mino time $\lambda \Rightarrow$ separate $\{r_p, \theta_p\}$ peridocity

$$r_p(\psi) = \frac{pM}{1+e\cos\psi} \qquad \cos\theta_p(\chi) = \sqrt{z_-}\cos\chi$$

$$\hat{C}^{\pm} = \int d\psi \int d\chi \tilde{A}^{\pm}(\psi,\chi)$$

- Separate into 1D integrals (for $s=0$)

$$\hat{C}^{\pm} = \int d\psi \tilde{F}_1^{\pm}(\psi)\int d\chi \tilde{F}_2(\chi) + \int d\psi \tilde{F}_3^{\pm}(\psi)\int d\chi \tilde{F}_4(\chi)$$

- Convert to discrete Fourier sums

$$\hat{C}^{\pm} = I_1^{\pm} I_2 + I_3^{\pm} I_4 \qquad \text{w/} \qquad I_1^{\pm} \sim \sum_{i=0}^{N_1-1} \tilde{F}_1^{\pm}(\psi_i)$$

- Numerical integration in 2D $\Rightarrow$ compute 4 1D Fourier sums

Computational efficiency of SSI on Kerr

- $a/M = 0.5$, $e = 0.5$, $p = 15$, $\iota = \pi/3$
- Calculate $C^{\pm}_{2222}$ mode

SSI on Kerr

Source integration on Kerr

$$\hat{C}^{\pm} = \frac{1}{W}\int_{r_{\min}}^{r_{\max}} \frac{\hat{X}^{\mp}(r)\tilde{\sigma}(r)(r^2+a^2)}{\Delta}\,dr$$

- Mino time $\lambda \Rightarrow$ separate $\{r_p, \theta_p\}$ peridocity

$$r_p(\psi) = \frac{pM}{1+e\cos\psi} \qquad \cos\theta_p(\chi) = \sqrt{z_-}\cos\chi$$

$$\hat{C}^{\pm} = \int d\psi \int d\chi \tilde{A}^{\pm}(\psi,\chi)$$

- Separate into 1D integrals (for $s=0$)

$$\hat{C}^{\pm} = \int d\psi \tilde{F}_1^{\pm}(\psi)\int d\chi \tilde{F}_2(\chi) + \int d\psi \tilde{F}_3^{\pm}(\psi)\int d\chi \tilde{F}_4(\chi)$$

- Convert to discrete Fourier sums

$$\hat{C}^{\pm} = I_1^{\pm} I_2 + I_3^{\pm} I_4 \qquad \text{w/} \qquad I_1^{\pm} \sim \sum_{i=0}^{N_1-1} \tilde{F}_1^{\pm}(\psi_i)$$

- Numerical integration in 2D $\Rightarrow$ compute 4 1D Fourier sums

Computational efficiency of SSI on Kerr

- $a/M = 0.5$, $e = 0.5$, $p = 15$, $\iota = \pi/3$
- Calculate $C^{\pm}_{2222}$ mode

SSI on Kerr

Source integration on Kerr

$$\hat{C}^{\pm} = \frac{1}{W}\int_{r_{\text{min}}}^{r_{\text{max}}} \frac{\hat{X}^{\mp}(r)\tilde{\sigma}(r)(r^2+a^2)}{\Delta}dr$$

- Mino time $\lambda \Rightarrow$ separate $\{r_p, \theta_p\}$ peridocity

$$r_p(\psi) = \frac{pM}{1+e\cos\psi} \qquad \cos\theta_p(\chi) = \sqrt{z_-}\cos\chi$$

$$\hat{C}^{\pm} = \int d\psi \int d\chi \tilde{A}^{\pm}(\psi,\chi)$$

- Separate into 1D integrals (for $s=0$)

$$\hat{C}^{\pm} = \int d\psi \tilde{F}_1^{\pm}(\psi)\int d\chi \tilde{F}_2(\chi) + \int d\psi \tilde{F}_3^{\pm}(\psi)\int d\chi \tilde{F}_4(\chi)$$

- Convert to discrete Fourier sums

$$\hat{C}^{\pm} = I_1^{\pm}I_2 + I_3^{\pm}I_4 \qquad \text{w/} \qquad I_1^{\pm} \sim \sum_{i=0}^{N_1-1}\tilde{F}_1^{\pm}(\psi_i)$$

- Numerical integration in 2D $\Rightarrow$ compute 4 1D Fourier sums

Computational efficiency of SSI on Kerr

- $a/M = 0.5$, $e = 0.5$, $p = 15$, $\iota = \pi/3$
- Calculate $C^{\pm}_{2222}$ mode

SSI on Kerr

Source integration on Kerr

$$\hat{C}^{\pm} = \frac{1}{W}\int_{r_{\min}}^{r_{\max}} \frac{\hat{X}^{\mp}(r)\tilde{\sigma}(r)(r^2+a^2)}{\Delta}dr$$

- Mino time $\lambda \Rightarrow$ separate $\{r_p, \theta_p\}$ peridocity

$$r_p(\psi) = \frac{pM}{1+e\cos\psi} \qquad \cos\theta_p(\chi) = \sqrt{z_-}\cos\chi$$

$$\hat{C}^{\pm} = \int d\psi \int d\chi \tilde{A}^{\pm}(\psi,\chi)$$

- Separate into 1D integrals (for $s=0$)

$$\hat{C}^{\pm} = \int d\psi \tilde{F}_1^{\pm}(\psi)\int d\chi \tilde{F}_2(\chi) + \int d\psi \tilde{F}_3^{\pm}(\psi)\int d\chi \tilde{F}_4(\chi)$$

- Convert to discrete Fourier sums

$$\hat{C}^{\pm} = I_1^{\pm}I_2 + I_3^{\pm}I_4 \qquad \text{w/} \qquad I_1^{\pm} \sim \sum_{i=0}^{N_1-1}\tilde{F}_1^{\pm}(\psi_i)$$

- Numerical integration in 2D $\Rightarrow$ compute 4 1D Fourier sums

Computational efficiency of SSI on Kerr

- $a/M = 0.5$, $e = 0.5$, $p = 15$, $\iota = \pi/3$
- Calculate $C_{2222}^{\pm}$ mode

Source integration on Kerr

$$\hat{C}^{\pm} = \frac{1}{W}\int_{r_{\min}}^{r_{\max}} \frac{\hat{X}^{\mp}(r)\tilde{\sigma}(r)(r^2+a^2)}{\Delta}dr$$

- Mino time $\lambda \Rightarrow$ separate $\{r_p, \theta_p\}$ peridocity

$$r_p(\psi) = \frac{pM}{1+e\cos\psi} \qquad \cos\theta_p(\chi) = \sqrt{z_-}\cos\chi$$

$$\hat{C}^{\pm} = \int d\psi \int d\chi \tilde{A}^{\pm}(\psi,\chi)$$

- Separate into 1D integrals (for $s=0$)

$$\hat{C}^{\pm} = \int d\psi \tilde{F}_1^{\pm}(\psi)\int d\chi \tilde{F}_2(\chi) + \int d\psi \tilde{F}_3^{\pm}(\psi)\int d\chi \tilde{F}_4(\chi)$$

- Convert to discrete Fourier sums

$$\hat{C}^{\pm} = I_1^{\pm} I_2 + I_3^{\pm} I_4 \qquad \text{w/} \qquad I_1^{\pm} \sim \sum_{i=0}^{N_1-1} \tilde{F}_1^{\pm}(\psi_i)$$

- Numerical integration in 2D $\Rightarrow$ compute 4 1D Fourier sums

Computational efficiency of SSI on Kerr

- $a/M = 0.5$, $e = 0.5$, $p = 15$, $\iota = \pi/3$
- Calculate $C^{\pm}_{2222}$ mode

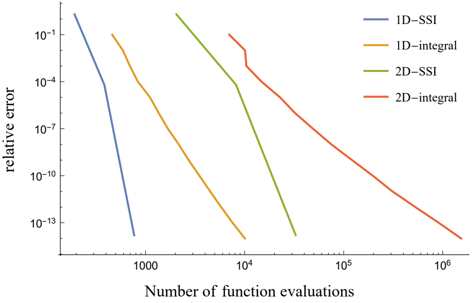

SSI on Kerr

Source integration on Kerr

$$\hat{C}^{\pm} = \frac{1}{W}\int_{r_{\min}}^{r_{\max}} \frac{\hat{X}^{\mp}(r)\tilde{\sigma}(r)(r^2+a^2)}{\Delta}\,dr$$

- Mino time $\lambda \Rightarrow$ separate $\{r_p, \theta_p\}$ peridocity

$$r_p(\psi) = \frac{pM}{1+e\cos\psi} \qquad \cos\theta_p(\chi) = \sqrt{z_-}\cos\chi$$

$$\hat{C}^{\pm} = \int d\psi \int d\chi \tilde{A}^{\pm}(\psi,\chi)$$

- Separate into 1D integrals (for $s=0$)

$$\hat{C}^{\pm} = \int d\psi \tilde{F}_1^{\pm}(\psi)\int d\chi \tilde{F}_2(\chi) + \int d\psi \tilde{F}_3^{\pm}(\psi)\int d\chi \tilde{F}_4(\chi)$$

- Convert to discrete Fourier sums

$$\hat{C}^{\pm} = I_1^{\pm} I_2 + I_3^{\pm} I_4 \qquad \text{w/} \qquad I_1^{\pm} \sim \sum_{i=0}^{N_1-1} \tilde{F}_1^{\pm}(\psi_i)$$

- Numerical integration in 2D $\Rightarrow$ compute 4 1D Fourier sums

Computational efficiency of SSI on Kerr

- $a/M = 0.5$, $e = 0.5$, $p = 15$, $\iota = \pi/3$
- Calculate $C^{\pm}_{2222}$ mode

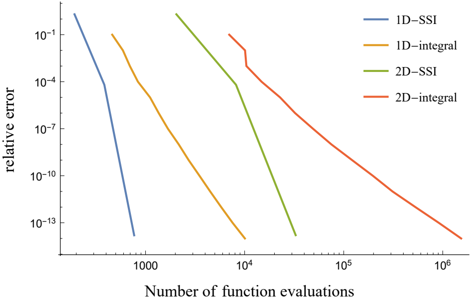

Computational efficiency improved by ~ 3 **orders of magnitude** for machine-precision

Flux Code Validation in the Equatorial Plane

Fluxes on Kerr

- Energy and angular momentum fluxes calculated from normalization coefficients

$$\langle \dot{\mathcal{E}}^{\pm} \rangle = \sum_{lmkn} f_m(\omega_{mkn}) |C^{\pm}_{lmkn}|^2 \qquad \mathcal{E} \to E \text{ or } L_z$$

Code and SSI Validation

- Reference values in Warburton & Barack (2011):
  $p = 10$, $e = 0.2$, $a/M = -0.5$, $\iota = 0$

Flux Code Validation in the Equatorial Plane

Fluxes on Kerr

- Energy and angular momentum fluxes calculated from normalization coefficients

$$\langle \dot{\mathcal{E}}^{\pm} \rangle = \sum_{lmkn} f_m(\omega_{mkn}) |C^{\pm}_{lmkn}|^2 \qquad \mathcal{E} \to E \text{ or } L_z$$

Code and SSI Validation

- Reference values in Warburton & Barack (2011):
  $p = 10$, $e = 0.2$, $a/M = -0.5$, $\iota = 0$

Flux Code Validation in the Equatorial Plane

Fluxes on Kerr

- Energy and angular momentum fluxes calculated from normalization coefficients

$$\langle \dot{\mathcal{E}}^{\pm} \rangle = \sum_{lmkn} f_m(\omega_{mkn}) |C^{\pm}_{lmkn}|^2 \qquad \mathcal{E} \to E \text{ or } L_z$$

Code and SSI Validation

- Reference values in Warburton & Barack (2011):
  $p = 10$, $e = 0.2$, $a/M = -0.5$, $\iota = 0$

Flux Code Validation in the Equatorial Plane

Fluxes on Kerr

- Energy and angular momentum fluxes calculated from normalization coefficients

$$\langle \dot{\mathcal{E}}^{\pm} \rangle = \sum_{lmkn} f_m(\omega_{mkn}) |C^{\pm}_{lmkn}|^2 \qquad \mathcal{E} \to E \text{ or } L_z$$

Code and SSI Validation

- Reference values in Warburton & Barack (2011):
  $p = 10$, $e = 0.2$, $a/M = -0.5$, $\iota = 0$

Flux Code Validation in the Equatorial Plane

Fluxes on Kerr

- Energy and angular momentum fluxes calculated from normalization coefficients

$$\langle \dot{\mathcal{E}}^{\pm} \rangle = \sum_{lmkn} f_m(\omega_{mkn}) |C^{\pm}_{lmkn}|^2 \qquad \mathcal{E} \to E \text{ or } L_z$$

Code and SSI Validation

- Reference values in Warburton & Barack (2011):
  $p = 10$, $e = 0.2$, $a/M = -0.5$, $\iota = 0$

Flux Code Validation in the Equatorial Plane

Fluxes on Kerr

- Energy and angular momentum fluxes calculated from normalization coefficients

$$\langle \dot{\mathcal{E}}^{\pm} \rangle = \sum_{lmkn} f_m(\omega_{mkn}) |C^{\pm}_{lmkn}|^2 \qquad \mathcal{E} \to E \text{ or } L_z$$

Code and SSI Validation

- Reference values in Warburton & Barack (2011):
$p = 10$, $e = 0.2$, $a/M = -0.5$, $\iota = 0$

$$\langle \dot{E} \rangle^{\text{tot}} = 3.6565609775 \times 10^{-5}$$

$$\langle \dot{L}_z \rangle^{\text{tot}} = 1.06932318967 \times 10^{-3}$$

Flux Code Validation in the Equatorial Plane

Fluxes on Kerr

- Energy and angular momentum fluxes calculated from normalization coefficients

$$\langle \dot{\mathcal{E}}^{\pm} \rangle = \sum_{lmkn} f_m(\omega_{mkn}) |C^{\pm}_{lmkn}|^2 \qquad \mathcal{E} \to E \text{ or } L_z$$

Code and SSI Validation

- Reference values in Warburton & Barack (2011):
  $p = 10$, $e = 0.2$, $a/M = -0.5$, $\iota = 0$

$$\langle \dot{E} \rangle^{\text{tot}} = 3.6565609775 \times 10^{-5}$$

$$\langle \dot{L}_z \rangle^{\text{tot}} = 1.06932318967 \times 10^{-3}$$

$$|1 - \langle \dot{E} \rangle^{\text{tot}} / \langle \dot{E} \rangle^{\text{ref}}| = 6.83703 \times 10^{-10}$$

$$|1 - \langle \dot{L}_z \rangle^{\text{tot}} / \langle \dot{L}_z \rangle^{\text{ref}}| = 3.13246 \times 10^{-10}$$

Flux Code Validation in the Equatorial Plane

Fluxes on Kerr

- Energy and angular momentum fluxes calculated from normalization coefficients

$$\langle \dot{\mathcal{E}}^{\pm} \rangle = \sum_{lmkn} f_m(\omega_{mkn}) |C^{\pm}_{lmkn}|^2 \qquad \mathcal{E} \to E \text{ or } L_z$$

Code and SSI Validation

- Reference values in Warburton & Barack (2011):
  $p = 10$, $e = 0.2$, $a/M = -0.5$, $\iota = 0$

$$\langle \dot{E} \rangle^{\text{tot}} = 3.6565609775 \times 10^{-5}$$

$$\langle \dot{L}_z \rangle^{\text{tot}} = 1.06932318967 \times 10^{-3}$$

$$|1 - \langle \dot{E} \rangle^{\text{tot}} / \langle \dot{E} \rangle^{\text{ref}}| = 6.83703 \times 10^{-10}$$

$$|1 - \langle \dot{L}_z \rangle^{\text{tot}} / \langle \dot{L}_z \rangle^{\text{ref}}| = 3.13246 \times 10^{-10}$$

$C^{\pm}$ & SSI for eccentric, equatorial Kerr

Flux Code Validation in the Equatorial Plane

Fluxes on Kerr

- Energy and angular momentum fluxes calculated from normalization coefficients

$$\langle \dot{\mathcal{E}}^{\pm} \rangle = \sum_{lmkn} f_m(\omega_{mkn}) |C^{\pm}_{lmkn}|^2 \qquad \mathcal{E} \to E \text{ or } L_z$$

Code and SSI Validation

- Reference values in Warburton & Barack (2011):
  $p = 10$, $e = 0.2$, $a/M = -0.5$, $\iota = 0$

$$\langle \dot{E} \rangle^{\text{tot}} = 3.6565609775 \times 10^{-5}$$

$$\langle \dot{L}_z \rangle^{\text{tot}} = 1.06932318967 \times 10^{-3}$$

$$|1 - \langle \dot{E} \rangle^{\text{tot}} / \langle \dot{E} \rangle^{\text{ref}}| = 6.83703 \times 10^{-10}$$
$$|1 - \langle \dot{L}_z \rangle^{\text{tot}} / \langle \dot{L}_z \rangle^{\text{ref}}| = 3.13246 \times 10^{-10}$$

$C^{\pm}$ & SSI for eccentric, equatorial Kerr ✓

Flux Code Self-Consistency

Inclined orbit on Schwarzschild

- Spherical symmetry $\Rightarrow$ physics should be unaffected by rotations

Equatorial case:

$p = 10$, $e = 0.2$, $a/M = 0$, $\iota = 0$
Sum over l, m, & n modes

Inclined case:

$p = 10$, $e = 0.2$, $a/M = 0$, $\iota = \pi/3$
Sum over l, m, k, & n modes

$\langle \dot{E} \rangle$ should have same value for both cases

Flux Code Self-Consistency

Inclined orbit on Schwarzschild

- Spherical symmetry $\Rightarrow$ physics should be unaffected by rotations

Equatorial case:

$p = 10$, $e = 0.2$, $a/M = 0$, $\iota = 0$
Sum over l, m, & n modes

Inclined case:

$p = 10$, $e = 0.2$, $a/M = 0$, $\iota = \pi/3$
Sum over l, m, k, & n modes

$\langle \dot{E} \rangle$ should have same value for both cases

Flux Code Self-Consistency

Inclined orbit on Schwarzschild

- Spherical symmetry $\Rightarrow$ physics should be unaffected by rotations

Equatorial case:

$p = 10$, $e = 0.2$, $a/M = 0$, $\iota = 0$
Sum over l, m, & n modes

Inclined case:

$p = 10$, $e = 0.2$, $a/M = 0$, $\iota = \pi/3$
Sum over l, m, k, & n modes

$\langle \dot{E} \rangle$ should have same value for both cases

Flux Code Self-Consistency

Inclined orbit on Schwarzschild

- Spherical symmetry $\Rightarrow$ physics should be unaffected by rotations

Equatorial case:

$p = 10$, $e = 0.2$, $a/M = 0$, $\iota = 0$

Sum over l, m, & n modes

Inclined case:

$p = 10$, $e = 0.2$, $a/M = 0$, $\iota = \pi/3$

Sum over l, m, k, & n modes

$\langle \dot{E} \rangle$ should have same value for both cases

Flux Code Self-Consistency

Inclined orbit on Schwarzschild

- Spherical symmetry $\Rightarrow$ physics should be unaffected by rotations

Equatorial case:

$p = 10,\ e = 0.2,\ a/M = 0,\ \iota = 0$
Sum over l, m, & n modes

Inclined case:

$p = 10,\ e = 0.2,\ a/M = 0,\ \iota = \pi/3$
Sum over l, m, k, & n modes

$\langle \dot{E} \rangle$ should have same value for both cases

Flux Code Self-Consistency

Inclined orbit on Schwarzschild

- Spherical symmetry $\Rightarrow$ physics should be unaffected by rotations

Equatorial case:

$p = 10$, $e = 0.2$, $a/M = 0$, $\iota = 0$
Sum over l, m, & n modes

Inclined case:

$p = 10$, $e = 0.2$, $a/M = 0$, $\iota = \pi/3$
Sum over l, m, k, & n modes

$\langle \dot{E} \rangle$ should have same value for both cases

Flux Code Self-Consistency

Inclined orbit on Schwarzschild

- Spherical symmetry $\Rightarrow$ physics should be unaffected by rotations

Equatorial case:

$p = 10$, $e = 0.2$, $a/M = 0$, $\iota = 0$
Sum over l, m, & n modes

Inclined case:

$p = 10$, $e = 0.2$, $a/M = 0$, $\iota = \pi/3$
Sum over l, m, k, & n modes

$\langle \dot{E} \rangle$ should have same value for both cases

Flux Code Self-Consistency

Inclined orbit on Schwarzschild

- Spherical symmetry $\Rightarrow$ physics should be unaffected by rotations

Equatorial case:

$p = 10,\ e = 0.2,\ a/M = 0,\ \iota = 0$
Sum over l, m, & n modes

Inclined case:

$p = 10,\ e = 0.2,\ a/M = 0,\ \iota = \pi/3$
Sum over l, m, k, & n modes

$\langle \dot{E} \rangle$ should have same value for both cases

$$\langle \dot{E} \rangle^{\text{inc}} = 3.21331398 \times 10^{-5}$$

$$|1 - \langle \dot{E} \rangle^{\text{inc}} / \langle \dot{E} \rangle^{\text{eq}}| = 2 \times 10^{-15}$$

Flux Code Self-Consistency

Inclined orbit on Schwarzschild

- Spherical symmetry $\Rightarrow$ physics should be unaffected by rotations

Equatorial case:

$p = 10,\ e = 0.2,\ a/M = 0,\ \iota = 0$
Sum over l, m, & n modes

Inclined case:

$p = 10,\ e = 0.2,\ a/M = 0,\ \iota = \pi/3$
Sum over l, m, k, & n modes

$\langle \dot{E} \rangle$ should have same value for both cases

$$\langle \dot{E} \rangle^{\text{inc}} = 3.21331398 \times 10^{-5}$$

$$|1 - \langle \dot{E} \rangle^{\text{inc}} / \langle \dot{E} \rangle^{\text{eq}}| = 2 \times 10^{-15}$$

Successful summation over
all 4 modes!

Flux Code Self-Consistency

Inclined orbit on Schwarzschild

- Spherical symmetry $\Rightarrow$ physics should be unaffected by rotations

Equatorial case:

$p = 10,\ e = 0.2,\ a/M = 0,\ \iota = 0$
Sum over l, m, & n modes

Inclined case:

$p = 10,\ e = 0.2,\ a/M = 0,\ \iota = \pi/3$
Sum over l, m, k, & n modes

$\langle \dot{E} \rangle$ should have same value for both cases

$$\langle \dot{E} \rangle^{\mathrm{inc}} = 3.21331398 \times 10^{-5}$$

$$|1 - \langle \dot{E} \rangle^{\mathrm{inc}} / \langle \dot{E} \rangle^{\mathrm{eq}}| = 2 \times 10^{-15}$$

Successful summation over all 4 modes!

$C^{\pm}$ & SSI for inclined, eccentric Schwarzschild

Flux Code Self-Consistency

Inclined orbit on Schwarzschild

- Spherical symmetry $\Rightarrow$ physics should be unaffected by rotations

Equatorial case:

$p = 10,\ e = 0.2,\ a/M = 0,\ \iota = 0$
Sum over l, m, & n modes

Inclined case:

$p = 10,\ e = 0.2,\ a/M = 0,\ \iota = \pi/3$
Sum over l, m, k, & n modes

$\langle \dot{E} \rangle$ should have same value for both cases

$$\langle \dot{E} \rangle^{\text{inc}} = 3.21331398 \times 10^{-5}$$

$$|1 - \langle \dot{E} \rangle^{\text{inc}} / \langle \dot{E} \rangle^{\text{eq}}| = 2 \times 10^{-15}$$

Successful summation over
all 4 modes!

$C^{\pm}$ & SSI for
inclined, eccentric ✓
Schwarzschild

SSF Code Validation in the Equatorial Plane

SSF of eccentric, equatorial orbit on Kerr

- $p = 10$, $e = 0.2$, $a/M = -0.5$, $\iota = 0$

SSF Code Validation in the Equatorial Plane

SSF of eccentric, equatorial orbit on Kerr

- $p = 10$, $e = 0.2$, $a/M = -0.5$, $\iota = 0$

SSF Code Validation in the Equatorial Plane

SSF of eccentric, equatorial orbit on Kerr

- $p = 10$, $e = 0.2$, $a/M = -0.5$, $\iota = 0$

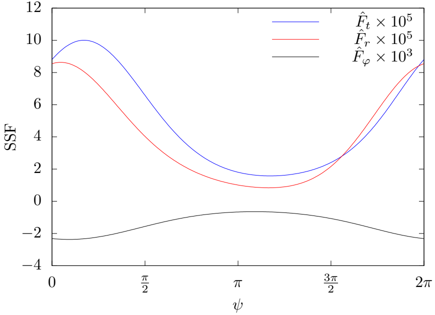

SSF Code Validation in the Equatorial Plane

SSF of eccentric, equatorial orbit on Kerr

- $p = 10$, $e = 0.2$, $a/M = -0.5$, $\iota = 0$

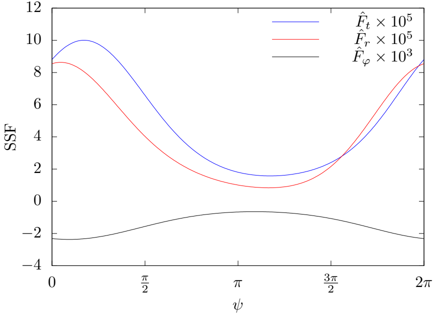

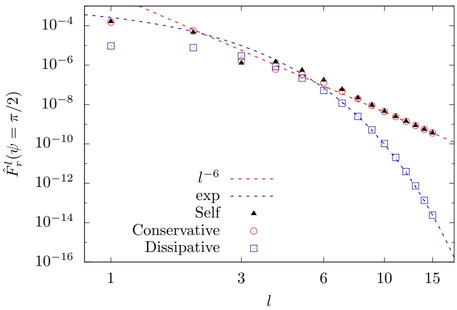

SSF Code Validation in the Equatorial Plane

SSF of eccentric, equatorial orbit on Kerr

- $p = 10,\ e = 0.2,\ a/M = -0.5,\ \iota = 0$

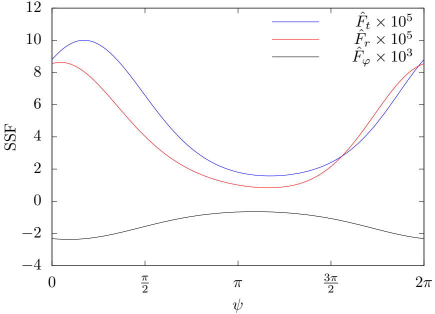

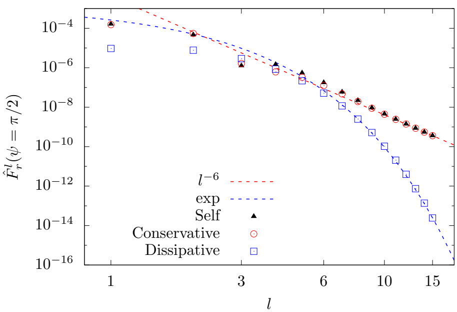

l^{-6} convergence w/ additional RPs from Heffernan et al.

SSF Code Validation in the Equatorial Plane

SSF of eccentric, equatorial orbit on Kerr

- $p = 10$, $e = 0.2$, $a/M = -0.5$, $\iota = 0$

	$F_t \times M^2/q^2$	$F_r \times M^2/q^2$	$F_\varphi \times M/q^2$
disp	4.5×10^{-5}	9.3×10^{-6}	-2.4×10^{-4}
cons	2.1×10^{-5}	3.1×10^{-5}	-1.3×10^{-3}

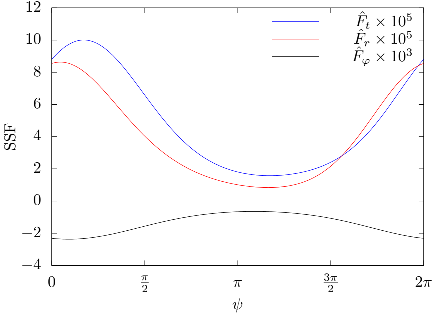

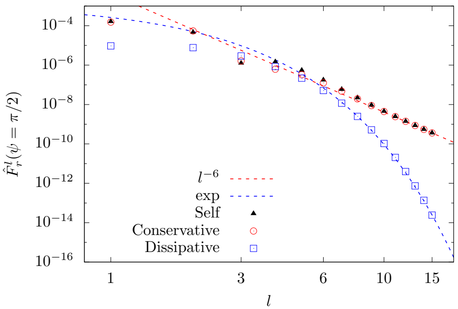

l^{-6} convergence w/ additional RPs from Heffernan et al.

SSF Code Validation in the Equatorial Plane

SSF of eccentric, equatorial orbit on Kerr

- $p = 10$, $e = 0.2$, $a/M = -0.5$, $\iota = 0$

	$F_t \times M^2/q^2$	$F_r \times M^2/q^2$	$F_\varphi \times M/q^2$
disp	3.3×10^{-9}	7.3×10^{-9}	4.0×10^{-9}
cons	2.4×10^{-5}	2.0×10^{-4}	5.2×10^{-5}

Relative Error with Warburton & Barack (2011)

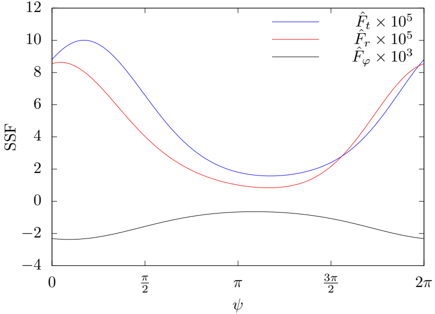

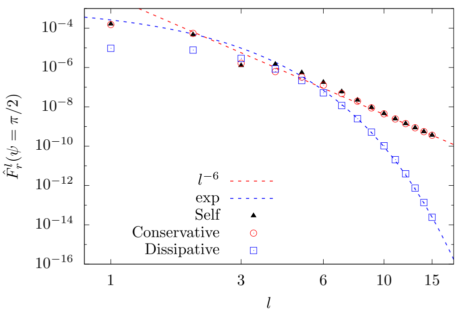

l^{-6} convergence w/ additional RPs from Heffernan et al.

SSF Code Validation in the Equatorial Plane

SSF of eccentric, equatorial orbit on Kerr

- $p = 10$, $e = 0.2$, $a/M = -0.5$, $\iota = 0$

	$F_t \times M^2/q^2$	$F_r \times M^2/q^2$	$F_\varphi \times M/q^2$
disp	3.3×10^{-9}	7.3×10^{-9}	4.0×10^{-9}
cons	2.4×10^{-5}	2.0×10^{-4}	5.2×10^{-5}

Relative Error with Warburton & Barack (2011)

SSF for eccentric, equatorial Kerr

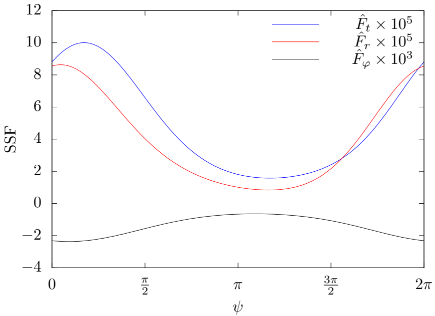

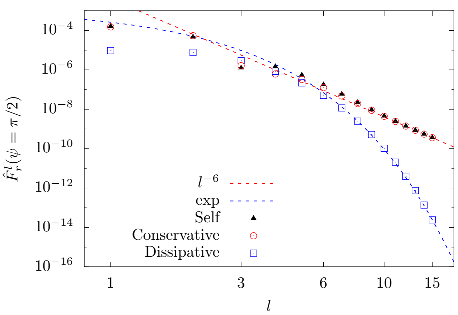

l^{-6} convergence w/ additional RPs from Heffernan et al.

SSF Code Validation in the Equatorial Plane

SSF of eccentric, equatorial orbit on Kerr

- $p = 10$, $e = 0.2$, $a/M = -0.5$, $\iota = 0$

	$F_t \times M^2/q^2$	$F_r \times M^2/q^2$	$F_\varphi \times M/q^2$
disp	3.3×10^{-9}	7.3×10^{-9}	4.0×10^{-9}
cons	2.4×10^{-5}	2.0×10^{-4}	5.2×10^{-5}

Relative Error with Warburton & Barack (2011)

SSF for eccentric, equatorial Kerr ✓

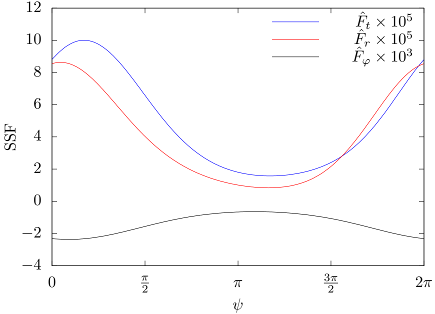

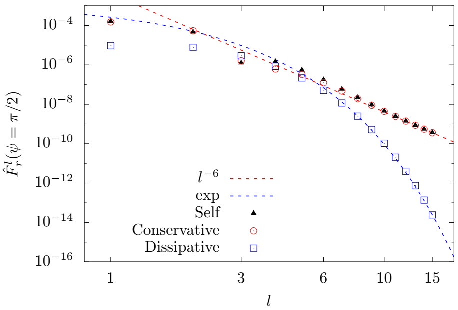

l^{-6} convergence w/ additional RPs from Heffernan et al.

SSF Code Self-Consistency

SSF over an eccentric, inclined orbit in Schwarzschild limit

Rotate coordinate system from equatorial case

$$F_t(\iota) = F_t^{\mathrm{eq}} \qquad F_\varphi(\iota) = F_\varphi^{\mathrm{eq}} \cos\iota$$

$$F_r(\iota) = F_r^{\mathrm{eq}} \qquad F_\theta(\iota) = \pm F_\varphi^{\mathrm{eq}} \cos\iota \sqrt{\sec^2\iota - \csc^2\theta_p}$$

Specify orbital parameters $p = 10$, $e = 0.2$, $a/M = 0$, $\iota = \pi/3$

SSF Code Self-Consistency

SSF over an eccentric, inclined orbit in Schwarzschild limit

Rotate coordinate system from equatorial case

$$F_t(\iota) = F_t^{\mathrm{eq}} \qquad F_\varphi(\iota) = F_\varphi^{\mathrm{eq}} \cos\iota$$

$$F_r(\iota) = F_r^{\mathrm{eq}} \qquad F_\theta(\iota) = \pm F_\varphi^{\mathrm{eq}} \cos\iota \sqrt{\sec^2\iota - \csc^2\theta_p}$$

Specify orbital parameters $p = 10$, $e = 0.2$, $a/M = 0$, $\iota = \pi/3$

SSF Code Self-Consistency

SSF over an eccentric, inclined orbit in Schwarzschild limit

Rotate coordinate system from equatorial case

$$F_t(\iota) = F_t^{\mathrm{eq}} \qquad F_\varphi(\iota) = F_\varphi^{\mathrm{eq}} \cos\iota$$

$$F_r(\iota) = F_r^{\mathrm{eq}} \qquad F_\theta(\iota) = \pm F_\varphi^{\mathrm{eq}} \cos\iota \sqrt{\sec^2\iota - \csc^2\theta_p}$$

Specify orbital parameters $p = 10$, $e = 0.2$, $a/M = 0$, $\iota = \pi/3$

SSF Code Self-Consistency

SSF over an eccentric, inclined orbit in Schwarzschild limit

Rotate coordinate system from equatorial case

$$F_t(\iota) = F_t^{\mathrm{eq}} \qquad F_\varphi(\iota) = F_\varphi^{\mathrm{eq}} \cos\iota$$

$$F_r(\iota) = F_r^{\mathrm{eq}} \qquad F_\theta(\iota) = \pm F_\varphi^{\mathrm{eq}} \cos\iota \sqrt{\sec^2\iota - \csc^2\theta_p}$$

Specify orbital parameters $p = 10$, $e = 0.2$, $a/M = 0$, $\iota = \pi/3$

SSF Code Self-Consistency

SSF over an eccentric, inclined orbit in Schwarzschild limit

Rotate coordinate system from equatorial case

$$F_t(\iota) = F_t^{\text{eq}} \qquad F_\varphi(\iota) = F_\varphi^{\text{eq}} \cos\iota$$

$$F_r(\iota) = F_r^{\text{eq}} \qquad F_\theta(\iota) = \pm F_\varphi^{\text{eq}} \cos\iota \sqrt{\sec^2\iota - \csc^2\theta_p}$$

Specify orbital parameters $p = 10$, $e = 0.2$, $a/M = 0$, $\iota = \pi/3$

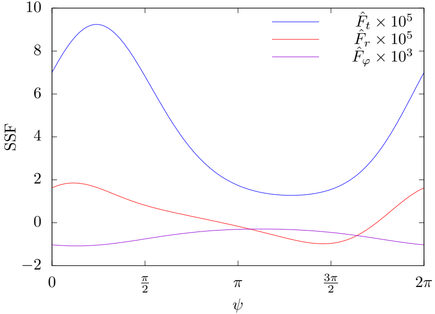

SSF Code Self-Consistency

SSF over an eccentric, inclined orbit in Schwarzschild limit

Rotate coordinate system from equatorial case

$$F_t(\iota) = F_t^{\mathrm{eq}} \qquad F_\varphi(\iota) = F_\varphi^{\mathrm{eq}} \cos\iota$$

$$F_r(\iota) = F_r^{\mathrm{eq}} \qquad F_\theta(\iota) = \pm F_\varphi^{\mathrm{eq}} \cos\iota \sqrt{\sec^2\iota - \csc^2\theta_p}$$

Specify orbital parameters $p = 10$, $e = 0.2$, $a/M = 0$, $\iota = \pi/3$

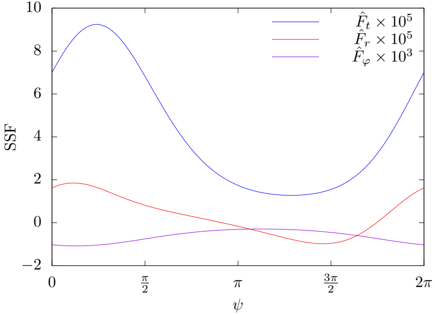

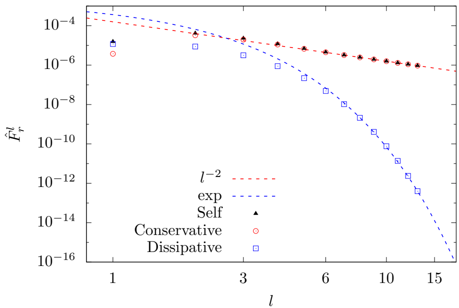

SSF Code Self-Consistency

SSF over an eccentric, inclined orbit in Schwarzschild limit

Rotate coordinate system from equatorial case

$$F_t(\iota) = F_t^{\rm eq} \qquad F_\varphi(\iota) = F_\varphi^{\rm eq}\cos\iota$$

$$F_r(\iota) = F_r^{\rm eq} \qquad F_\theta(\iota) = \pm F_\varphi^{\rm eq}\cos\iota\sqrt{\sec^2\iota - \csc^2\theta_p}$$

Specify orbital parameters $p = 10$, $e = 0.2$, $a/M = 0$, $\iota = \pi/3$

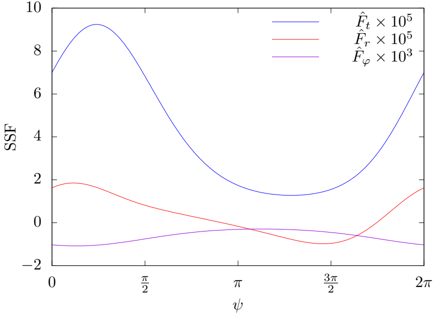

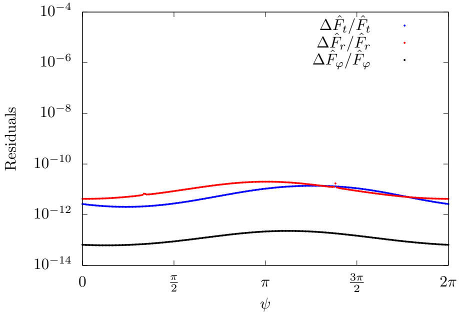

SSF Code Self-Consistency

SSF over an eccentric, inclined orbit in Schwarzschild limit

Rotate coordinate system from equatorial case

$$F_t(\iota) = F_t^{\mathrm{eq}} \qquad F_\varphi(\iota) = F_\varphi^{\mathrm{eq}} \cos\iota$$

$$F_r(\iota) = F_r^{\mathrm{eq}} \qquad F_\theta(\iota) = \pm F_\varphi^{\mathrm{eq}} \cos\iota \sqrt{\sec^2\iota - \csc^2\theta_p}$$

SSF for inclined, eccentric Schwarzschild

Specify orbital parameters $p = 10$, $e = 0.2$, $a/M = 0$, $\iota = \pi/3$

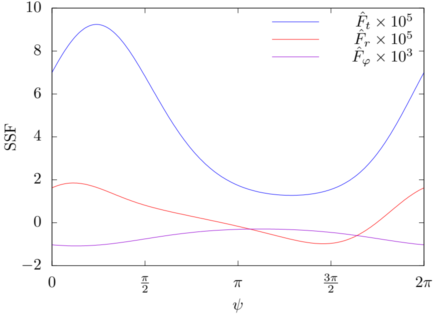

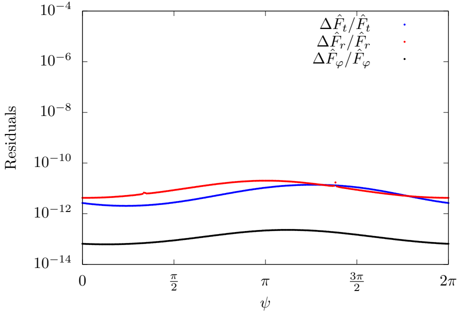

SSF Code Self-Consistency

SSF over an eccentric, inclined orbit in Schwarzschild limit

Rotate coordinate system from equatorial case

$$F_t(\iota) = F_t^{\mathrm{eq}} \qquad F_\varphi(\iota) = F_\varphi^{\mathrm{eq}} \cos\iota$$

$$F_r(\iota) = F_r^{\mathrm{eq}} \qquad F_\theta(\iota) = \pm F_\varphi^{\mathrm{eq}} \cos\iota \sqrt{\sec^2\iota - \csc^2\theta_p}$$

SSF for inclined, eccentric Schwarzschild ✓

Specify orbital parameters $p = 10$, $e = 0.2$, $a/M = 0$, $\iota = \pi/3$

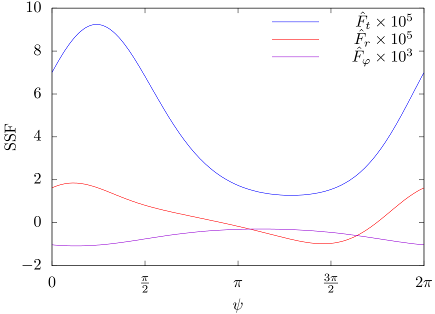

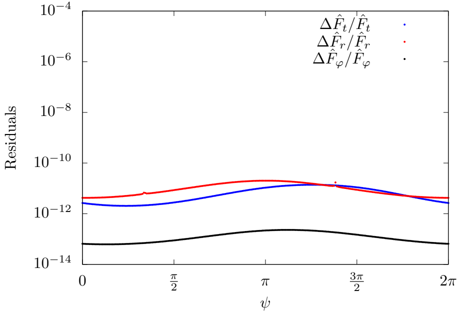

SSF Code Self-Consistency

SSF over an eccentric, inclined orbit in Schwarzschild limit

Rotate coordinate system from equatorial case

$$F_t(\iota) = F_t^{\mathrm{eq}} \qquad F_\varphi(\iota) = F_\varphi^{\mathrm{eq}} \cos\iota$$

$$F_r(\iota) = F_r^{\mathrm{eq}} \qquad F_\theta(\iota) = \pm F_\varphi^{\mathrm{eq}} \cos\iota \sqrt{\sec^2\iota - \csc^2\theta_p}$$

SSF for inclined, eccentric Schwarzschild ✓*

Specify orbital parameters $p = 10$, $e = 0.2$, $a/M = 0$, $\iota = \pi/3$

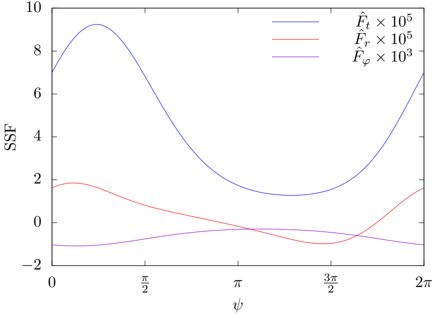

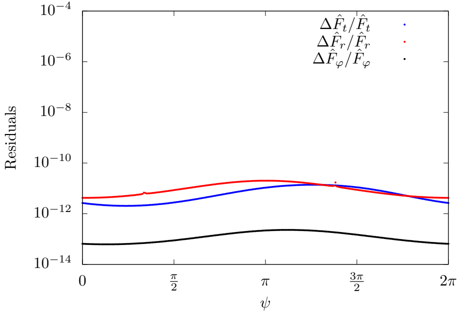

SSF Code for Eccentric, Inclined Orbit - NEW RESULTS!

SSF of eccentric, inclined orbit on Kerr

- $p = 7.6125$, $e = 0.1$, $a/M = 0.1$, $\iota = 0.3927 \approx \pi/8$

SSF Code for Eccentric, Inclined Orbit - NEW RESULTS!

SSF of eccentric, inclined orbit on Kerr

- $p = 7.6125$, $e = 0.1$, $a/M = 0.1$, $\iota = 0.3927 \approx \pi/8$

SSF of eccentric, inclined orbit on Kerr

- $p = 7.6125$, $e = 0.1$, $a/M = 0.1$, $\iota = 0.3927 \approx \pi/8$

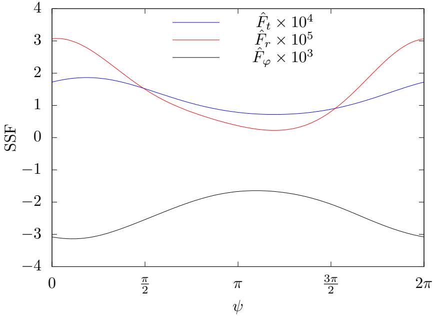

SSF Code for Eccentric, Inclined Orbit - NEW RESULTS!

SSF of eccentric, inclined orbit on Kerr

- $p = 7.6125$, $e = 0.1$, $a/M = 0.1$, $\iota = 0.3927 \approx \pi/8$

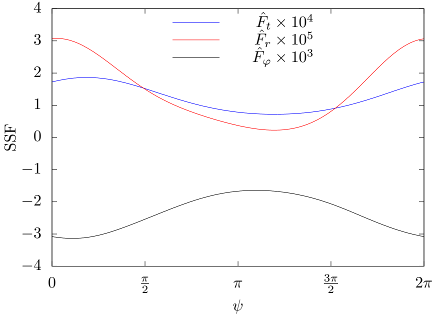

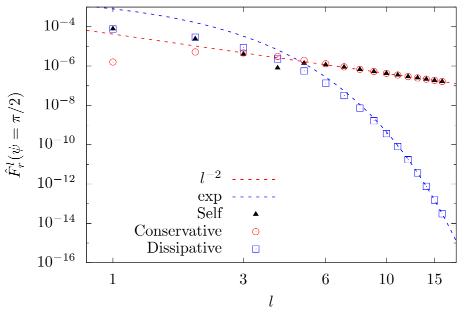

SSF Code for Eccentric, Inclined Orbit - NEW RESULTS!

SSF of eccentric, inclined orbit on Kerr $\Longrightarrow$ (Low) resonant orbit: $\Omega_\theta = 2\Omega_r$

- $p = 7.6125$, $e = 0.1$, $a/M = 0.1$, $\iota = 0.3927 \approx \pi/8$

Balance fluxes with E & L_z dissipated by SSF

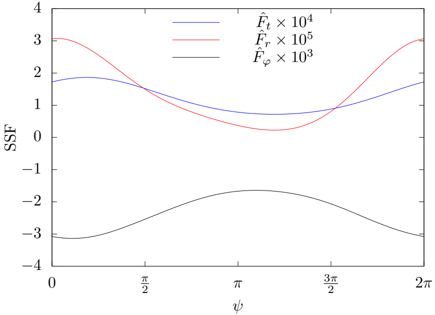

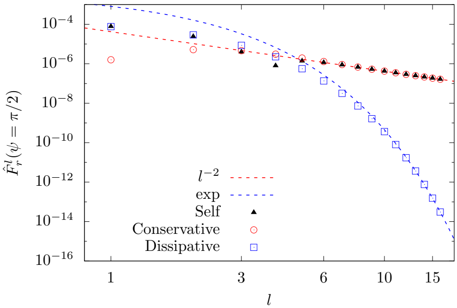

SSF Code for Eccentric, Inclined Orbit - NEW RESULTS!

SSF of eccentric, inclined orbit on Kerr $\Longrightarrow$ (Low) resonant orbit: $\Omega_\theta = 2\Omega_r$

- $p = 7.6125$, $e = 0.1$, $a/M = 0.1$, $\iota = 0.3927 \approx \pi/8$

Balance fluxes with E & L_z dissipated by SSF

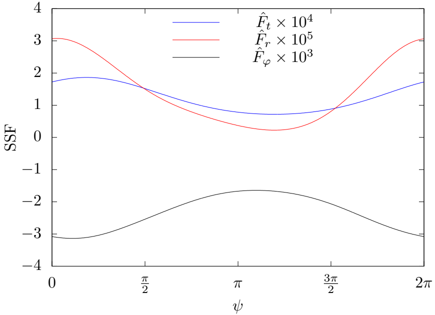

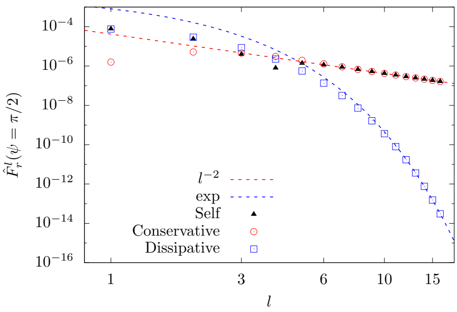

SSF Code for Eccentric, Inclined Orbit - NEW RESULTS!

SSF of eccentric, inclined orbit on Kerr $\Longrightarrow$ (Low) resonant orbit: $\Omega_\theta = 2\Omega_r$

- $p = 7.6125,\ e = 0.1,\ a/M = 0.1,\ \iota = 0.3927 \approx \pi/8$

Balance fluxes with E & L_z dissipated by SSF

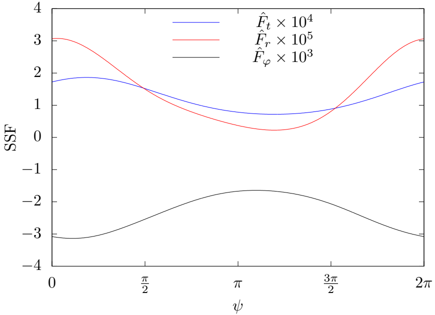

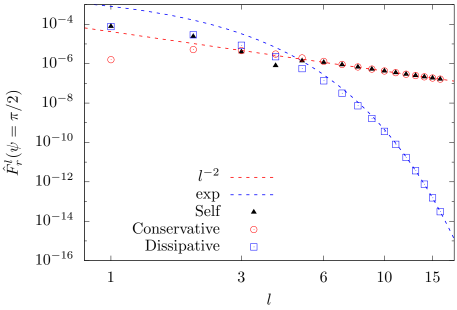

$$\langle \dot{E} \rangle^{\text{tot}} = \langle \dot{E}^{\text{hor}} \rangle + \langle \dot{E}^{\infty} \rangle$$

SSF Code for Eccentric, Inclined Orbit - NEW RESULTS!

SSF of eccentric, inclined orbit on Kerr $\Longrightarrow$ (Low) resonant orbit: $\Omega_\theta = 2\Omega_r$

- $p = 7.6125$, $e = 0.1$, $a/M = 0.1$, $\iota = 0.3927 \approx \pi/8$

Balance fluxes with E & L_z dissipated by SSF

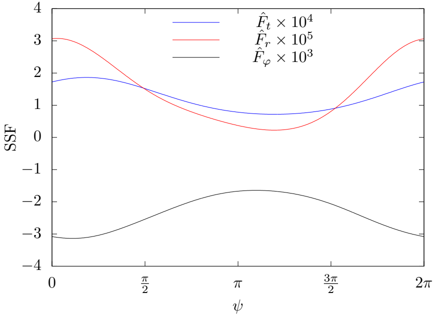

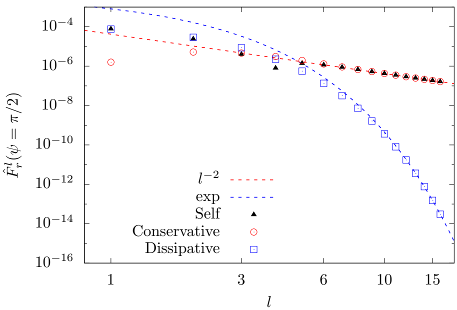

$$\langle \dot{E} \rangle^{\text{tot}} = \langle \dot{E}^{\text{hor}} \rangle + \langle \dot{E}^{\infty} \rangle$$

$$\langle \mathcal{W} \rangle = \frac{1}{T_r} \int_0^{T_r} \frac{F_t(t)}{u^t} dt - \mathcal{E} \Delta\mu$$

$$\langle \mathcal{T} \rangle = -\frac{1}{T_r} \int_0^{T_r} \frac{F_\varphi(t)}{u^t} dt + \mathcal{L}_z \Delta\mu$$

SSF Code for Eccentric, Inclined Orbit - NEW RESULTS!

SSF of eccentric, inclined orbit on Kerr $\Longrightarrow$ (Low) resonant orbit: $\Omega_\theta = 2\Omega_r$

- $p = 7.6125$, $e = 0.1$, $a/M = 0.1$, $\iota = 0.3927 \approx \pi/8$

Balance fluxes with E & L_z dissipated by SSF

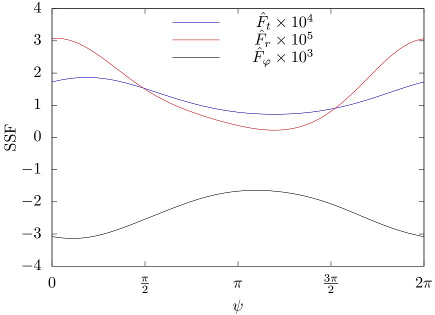

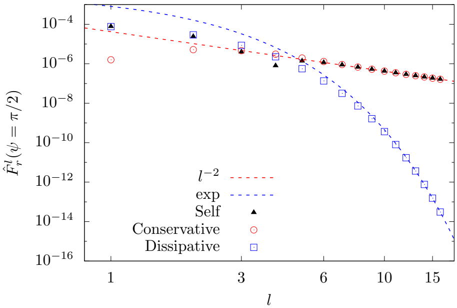

$$\langle \dot{E} \rangle^{\text{tot}} = \langle \dot{E}^{\text{hor}} \rangle + \langle \dot{E}^{\infty} \rangle$$

$$\langle \mathcal{W} \rangle = \frac{1}{T_r} \int_0^{T_r} \frac{F_t(t)}{u^t} dt - \mathcal{E}\Delta\mu$$

$$\langle \mathcal{T} \rangle = -\frac{1}{T_r} \int_0^{T_r} \frac{F_\varphi(t)}{u^t} dt + \mathcal{L}_z\Delta\mu$$

$$\langle \dot{E} \rangle^{\text{tot}} = 9.3148390367 \times 10^{-5} \qquad \langle \dot{L}_z \rangle^{\text{tot}} = 1.78925709 \times 10^{-3}$$

$$\langle \mathcal{W} \rangle = 9.3148390361 \times 10^{-5} \qquad \langle \mathcal{T} \rangle = 1.789257112 \times 10^{-3}$$

SSF Code for Eccentric, Inclined Orbit - NEW RESULTS!

SSF of eccentric, inclined orbit on Kerr $\Longrightarrow$ (Low) resonant orbit: $\Omega_\theta = 2\Omega_r$

- $p = 7.6125$, $e = 0.1$, $a/M = 0.1$, $\iota = 0.3927 \approx \pi/8$

Balance fluxes with E & L_z dissipated by SSF

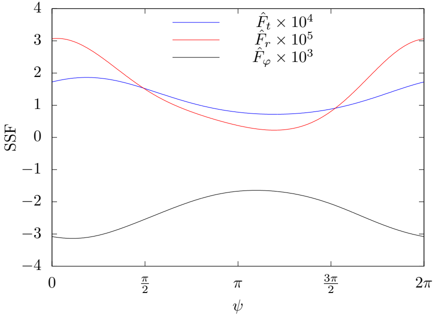

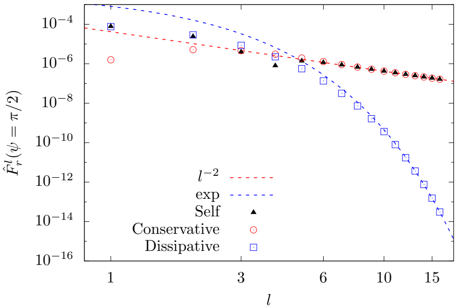

$$\langle \dot{E} \rangle^{\text{tot}} = \langle \dot{E}^{\text{hor}} \rangle + \langle \dot{E}^{\infty} \rangle$$

$$\langle \mathcal{W} \rangle = \frac{1}{T_r} \int_0^{T_r} \frac{F_t(t)}{u^t} dt - \mathcal{E}\Delta\mu$$

$$\langle \mathcal{T} \rangle = -\frac{1}{T_r} \int_0^{T_r} \frac{F_\varphi(t)}{u^t} dt + \mathcal{L}_z\Delta\mu$$

$$\langle \dot{E} \rangle^{\text{tot}} = 9.3148390367 \times 10^{-5} \qquad \langle \dot{L}_z \rangle^{\text{tot}} = 1.78925709 \times 10^{-3}$$

$$\langle \mathcal{W} \rangle = 9.3148390361 \times 10^{-5} \qquad \langle \mathcal{T} \rangle = 1.789257112 \times 10^{-3}$$

$$\left| 1 - \langle \mathcal{W} \rangle / \langle \dot{E} \rangle^{\text{tot}} \right| = 5.68 \times 10^{-11} \qquad \left| 1 - \langle \mathcal{T} \rangle / \langle \dot{L}_z \rangle^{\text{tot}} \right| = 1.03 \times 10^{-8}$$

SSF of eccentric, inclined orbit on Kerr $\Longrightarrow$ (Low) resonant orbit: $\Omega_\theta = 2\Omega_r$

- $p = 7.6125,\ e = 0.1,\ a/M = 0.1,\ \iota = 0.3927 \approx \pi/8$

Balance fluxes with E & L_z dissipated by SSF

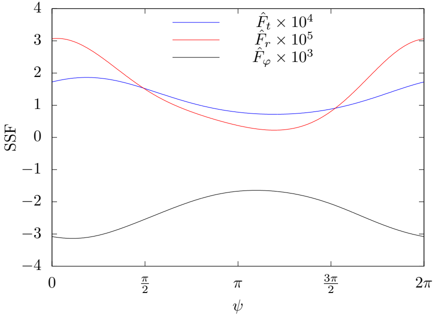

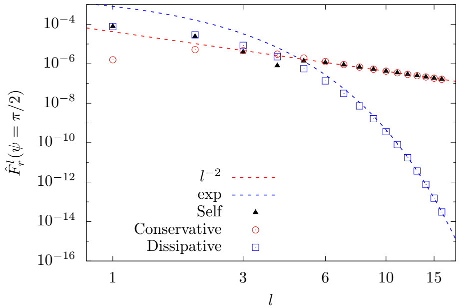

$$\langle \dot{E} \rangle^{\text{tot}} = \langle \dot{E}^{\text{hor}} \rangle + \langle \dot{E}^{\infty} \rangle$$

$$\langle \mathcal{W} \rangle = \frac{1}{T_r} \int_0^{T_r} \frac{F_t(t)}{u^t} dt - \mathcal{E} \Delta\mu$$

$$\langle \mathcal{T} \rangle = -\frac{1}{T_r} \int_0^{T_r} \frac{F_\varphi(t)}{u^t} dt + \mathcal{L}_z \Delta\mu$$

$$\langle \dot{E} \rangle^{l\max} / \langle \dot{E} \rangle^{\text{tot}} = 5.45 \times 10^{-12} \qquad \langle \dot{L}_z \rangle^{l\max} / \langle \dot{L}_z \rangle^{\text{tot}} = 4.94 \times 10^{-12}$$

$$\textsc{Max}\left[F_t^{\bar{l}\max} / F_t \right] = 4.65 \times 10^{-9} \qquad \textsc{Max}\left[F_\varphi^{\bar{l}\max} / F_\varphi \right] = 4.23 \times 10^{-9}$$

$$\left| 1 - \langle \mathcal{W} \rangle / \langle \dot{E} \rangle^{\text{tot}} \right| = 5.68 \times 10^{-11} \qquad \left| 1 - \langle \mathcal{T} \rangle / \langle \dot{L}_z \rangle^{\text{tot}} \right| = 1.03 \times 10^{-8}$$

Conclusions

Successfully implemented SSF code for inclined, eccentric orbits on Kerr

- Extends SSI techniques to Kerr spacetime
- Can handle arbitrary numerical precision
  - Mathematica, MST, SSI
- Confirmed previous results in literature
- Produced self-consistent (equatorial vs. inclined) results in Schwarzschild limit ($a \to 0$)
- Resonant orbits provide new, self-consistent (energy flux vs. work) results for generic orbits in Kerr spacetime

Moving forward

- Incorporate regularization scheme for F_θ
- Probe higher eccentricities and spins

Conclusions

Successfully implemented SSF code for inclined, eccentric orbits on Kerr

- Extends SSI techniques to Kerr spacetime
- Can handle arbitrary numerical precision
  - Mathematica, MST, SSI
- Confirmed previous results in literature
- Produced self-consistent (equatorial vs. inclined) results in Schwarzschild limit ($a \to 0$)
- Resonant orbits provide new, self-consistent (energy flux vs. work) results for generic orbits in Kerr spacetime

Moving forward

- Incorporate regularization scheme for F_θ
- Probe higher eccentricities and spins

Conclusions

Successfully implemented SSF code for inclined, eccentric orbits on Kerr

- Extends SSI techniques to Kerr spacetime
- Can handle arbitrary numerical precision
  - Mathematica, MST, SSI
- Confirmed previous results in literature
- Produced self-consistent (equatorial vs. inclined) results in Schwarzschild limit ($a \to 0$)
- Resonant orbits provide new, self-consistent (energy flux vs. work) results for generic orbits in Kerr spacetime

Moving forward

- Incorporate regularization scheme for F_θ
- Probe higher eccentricities and spins

Conclusions

Successfully implemented SSF code for inclined, eccentric orbits on Kerr

- Extends SSI techniques to Kerr spacetime
- Can handle arbitrary numerical precision
    - Mathematica, MST, SSI
- Confirmed previous results in literature
- Produced self-consistent (equatorial vs. inclined) results in Schwarzschild limit ($a \to 0$)
- Resonant orbits provide new, self-consistent (energy flux vs. work) results for generic orbits in Kerr spacetime

Moving forward

- Incorporate regularization scheme for F_θ
- Probe higher eccentricities and spins

Conclusions

Successfully implemented SSF code for inclined, eccentric orbits on Kerr

- Extends SSI techniques to Kerr spacetime
- Can handle arbitrary numerical precision
  - Mathematica, MST, SSI
- Confirmed previous results in literature
- Produced self-consistent (equatorial vs. inclined) results in Schwarzschild limit ($a \to 0$)
- Resonant orbits provide new, self-consistent (energy flux vs. work) results for generic orbits in Kerr spacetime

Moving forward

- Incorporate regularization scheme for F_θ
- Probe higher eccentricities and spins

Conclusions

Successfully implemented SSF code for inclined, eccentric orbits on Kerr

- Extends SSI techniques to Kerr spacetime
- Can handle arbitrary numerical precision
  - Mathematica, MST, SSI
- Confirmed previous results in literature
- Produced self-consistent (equatorial vs. inclined) results in Schwarzschild limit ($a \to 0$)
- Resonant orbits provide new, self-consistent (energy flux vs. work) results for generic orbits in Kerr spacetime

Moving forward

- Incorporate regularization scheme for F_θ
- Probe higher eccentricities and spins

Conclusions

Successfully implemented SSF code for inclined, eccentric orbits on Kerr

- Extends SSI techniques to Kerr spacetime
- Can handle arbitrary numerical precision
  - Mathematica, MST, SSI
- Confirmed previous results in literature
- Produced self-consistent (equatorial vs. inclined) results in Schwarzschild limit ($a \to 0$)
- Resonant orbits provide new, self-consistent (energy flux vs. work) results for generic orbits in Kerr spacetime

Moving forward

- Incorporate regularization scheme for F_θ
- Probe higher eccentricities and spins

Conclusions

Successfully implemented SSF code for inclined, eccentric orbits on Kerr

- Extends SSI techniques to Kerr spacetime
- Can handle arbitrary numerical precision
    - Mathematica, MST, SSI
- Confirmed previous results in literature
- Produced self-consistent (equatorial vs. inclined) results in Schwarzschild limit ($a \to 0$)
- Resonant orbits provide new, self-consistent (energy flux vs. work) results for generic orbits in Kerr spacetime

Moving forward

- Incorporate regularization scheme for F_θ
- Probe higher eccentricities and spins

Conclusions

Successfully implemented SSF code for inclined, eccentric orbits on Kerr

- Extends SSI techniques to Kerr spacetime
- Can handle arbitrary numerical precision
  - MATHEMATICA, MST, SSI
- Confirmed previous results in literature
- Produced self-consistent (equatorial vs. inclined) results in Schwarzschild limit ($a \to 0$)
- Resonant orbits provide new, self-consistent (energy flux vs. work) results for generic orbits in Kerr spacetime

Moving forward

- Incorporate regularization scheme for F_θ
- Probe higher eccentricities and spins

Conclusions

Successfully implemented SSF code for inclined, eccentric orbits on Kerr

- Extends SSI techniques to Kerr spacetime
- Can handle arbitrary numerical precision
  - Mathematica, MST, SSI
- Confirmed previous results in literature
- Produced self-consistent (equatorial vs. inclined) results in Schwarzschild limit ($a \to 0$)
- Resonant orbits provide new, self-consistent (energy flux vs. work) results for generic orbits in Kerr spacetime

Moving forward

- Incorporate regularization scheme for F_θ
- Probe higher eccentricities and spins

Questions?

MST analytic function expansion overview

Use Mano, Suzuki, and Takasugi (1996) (MST) method (earlier Leaver)

- $R^{\rm in}_{lm\omega}$ is an expansion (a_n) in hypergeometric functions $p_{n+\nu}$

$$R^{\rm in}_{lm\omega} = e^{-i\omega r_*}\, r^2\, k(r) \sum_{n=-\infty}^{\infty} a_n p_{n+\nu}(r)$$

- Outer solution $R^{\rm up}_{lm\omega}$ from expansion (b_n) in Coulomb wave functions

Free parameter: the renormalized angular momentum ν

- Eigenvalue of ν makes recurrence for a_n and b_n convergent $n \to \pm\infty$

Well understood procedure [see Sasaki & Tagoshi (2006) (LRR)]

Implemented in MATHEMATICA $\to$ arbitrary precision calculations

MST analytic function expansion overview

Use Mano, Suzuki, and Takasugi (1996) (MST) method (earlier Leaver)

- $R^{\text{in}}_{lm\omega}$ is an expansion (a_n) in hypergeometric functions $p_{n+\nu}$

$$R^{\text{in}}_{lm\omega} = e^{-i\omega r_*}\, r^2\, k(r) \sum_{n=-\infty}^{\infty} a_n p_{n+\nu}(r)$$

- Outer solution $R^{\text{up}}_{lm\omega}$ from expansion (b_n) in Coulomb wave functions

Free parameter: the renormalized angular momentum ν

- Eigenvalue of ν makes recurrence for a_n and b_n convergent $n \to \pm\infty$

Well understood procedure [see Sasaki & Tagoshi (2006) (LRR)]

Implemented in Mathematica $\to$ arbitrary precision calculations

MST analytic function expansion overview

Use Mano, Suzuki, and Takasugi (1996) (MST) method (earlier Leaver)

- $R^{\rm in}_{lm\omega}$ is an expansion (a_n) in hypergeometric functions $p_{n+\nu}$

$$R^{\rm in}_{lm\omega} = e^{-i\omega r_*}\, r^2\, k(r) \sum_{n=-\infty}^{\infty} a_n p_{n+\nu}(r)$$

- Outer solution $R^{\rm up}_{lm\omega}$ from expansion (b_n) in Coulomb wave functions

Free parameter: the renormalized angular momentum ν

- Eigenvalue of ν makes recurrence for a_n and b_n convergent $n \to \pm\infty$

Well understood procedure [see Sasaki & Tagoshi (2006) (LRR)]

Implemented in MATHEMATICA $\to$ arbitrary precision calculations

MST analytic function expansion overview

Use Mano, Suzuki, and Takasugi (1996) (MST) method (earlier Leaver)

- $R^{\mathrm{in}}_{lm\omega}$ is an expansion (a_n) in hypergeometric functions $p_{n+\nu}$

$$R^{\mathrm{in}}_{lm\omega} = e^{-i\omega r_*}\, r^2\, k(r) \sum_{n=-\infty}^{\infty} a_n p_{n+\nu}(r)$$

- Outer solution $R^{\mathrm{up}}_{lm\omega}$ from expansion (b_n) in Coulomb wave functions

Free parameter: the renormalized angular momentum ν

- Eigenvalue of ν makes recurrence for a_n and b_n convergent $n \to \pm\infty$

Well understood procedure [see Sasaki & Tagoshi (2006) (LRR)]

Implemented in MATHEMATICA $\to$ arbitrary precision calculations

MST analytic function expansion overview

Use Mano, Suzuki, and Takasugi (1996) (MST) method (earlier Leaver)

- $R^{\rm in}_{lm\omega}$ is an expansion (a_n) in hypergeometric functions $p_{n+\nu}$

$$R^{\rm in}_{lm\omega} = e^{-i\omega r_*}\, r^2\, k(r) \sum_{n=-\infty}^{\infty} a_n p_{n+\nu}(r)$$

- Outer solution $R^{\rm up}_{lm\omega}$ from expansion (b_n) in Coulomb wave functions

Free parameter: the renormalized angular momentum ν

- Eigenvalue of ν makes recurrence for a_n and b_n convergent $n \to \pm\infty$

Well understood procedure [see Sasaki & Tagoshi (2006) (LRR)]

Implemented in MATHEMATICA $\to$ arbitrary precision calculations

MST analytic function expansion overview

Use Mano, Suzuki, and Takasugi (1996) (MST) method (earlier Leaver)

- $R^{\text{in}}_{lm\omega}$ is an expansion (a_n) in hypergeometric functions $p_{n+\nu}$

$$R^{\text{in}}_{lm\omega} = e^{-i\omega r_*}\, r^2\, k(r) \sum_{n=-\infty}^{\infty} a_n p_{n+\nu}(r)$$

- Outer solution $R^{\text{up}}_{lm\omega}$ from expansion (b_n) in Coulomb wave functions

Free parameter: the renormalized angular momentum ν

- Eigenvalue of ν makes recurrence for a_n and b_n convergent $n \to \pm\infty$

Well understood procedure [see Sasaki & Tagoshi (2006) (LRR)]

Implemented in Mathematica $\to$ arbitrary precision calculations

Components of the self-force

Conservative and dissipative components

$$F_\alpha^{\text{cons}}(\tau) = \frac{1}{2}\left[F_\alpha^{(\text{full})}(\tau) + \epsilon_{(\alpha)} F_\alpha^{(\text{full})}(-\tau)\right] \qquad \longleftarrow \qquad \text{perturbs orbital parameters, exponential convergence}$$

$$F_\alpha^{\text{disp}}(\tau) = \frac{1}{2}\left[F_\alpha^{(\text{full})}(\tau) - \epsilon_{(\alpha)} F_\alpha^{(\text{full})}(-\tau)\right] \qquad \longleftarrow \qquad \text{radiation reaction, algebraic convergence}$$

Fiducial geodesics: $(t_p, r_p, \theta_p, \varphi_p) \to (-t_p, r_p, \theta_p, -\varphi_p)$

Components of the self-force

Conservative and dissipative components

$$F_\alpha^{\text{cons}}(\tau) = \frac{1}{2}\left[F_\alpha^{(\text{full})}(\tau) + \epsilon_{(\alpha)} F_\alpha^{(\text{full})}(-\tau)\right] \qquad \longleftarrow \qquad \text{perturbs orbital parameters, exponential convergence}$$

$$F_\alpha^{\text{disp}}(\tau) = \frac{1}{2}\left[F_\alpha^{(\text{full})}(\tau) - \epsilon_{(\alpha)} F_\alpha^{(\text{full})}(-\tau)\right] \qquad \longleftarrow \qquad \text{radiation reaction, algebraic convergence}$$

Fiducial geodesics: $(t_p, r_p, \theta_p, \varphi_p) \to (-t_p, r_p, \theta_p, -\varphi_p)$

Components of the self-force

Conservative and dissipative components

$$F_\alpha^{\rm cons}(\tau) = \frac{1}{2}\left[F_\alpha^{\rm (full)}(\tau) + \epsilon_{(\alpha)} F_\alpha^{\rm (full)}(-\tau)\right] \qquad \longleftarrow \qquad \text{perturbs orbital parameters, exponential convergence}$$

$$F_\alpha^{\rm disp}(\tau) = \frac{1}{2}\left[F_\alpha^{\rm (full)}(\tau) - \epsilon_{(\alpha)} F_\alpha^{\rm (full)}(-\tau)\right] \qquad \longleftarrow \qquad \text{radiation reaction, algebraic convergence}$$

Fiducial geodesics: $(t_p, r_p, \theta_p, \varphi_p) \to (-t_p, r_p, \theta_p, -\varphi_p)$

Components of the self-force

Conservative and dissipative components

$$F_\alpha^{\text{cons}}(\tau) = \frac{1}{2}\left[F_\alpha^{(\text{full})}(\tau) + \epsilon_{(\alpha)} F_\alpha^{(\text{full})}(-\tau)\right] \qquad \longleftarrow \qquad \text{perturbs orbital parameters, exponential convergence}$$

$$F_\alpha^{\text{disp}}(\tau) = \frac{1}{2}\left[F_\alpha^{(\text{full})}(\tau) - \epsilon_{(\alpha)} F_\alpha^{(\text{full})}(-\tau)\right] \qquad \longleftarrow \qquad \text{radiation reaction, algebraic convergence}$$

Fiducial geodesics: $(t_p, r_p, \theta_p, \varphi_p) \to (-t_p, r_p, \theta_p, -\varphi_p)$